Contrib Mineral Petrol (2004) 146: 546–565
DOI 10.1007/s00410-003-0520-8

ORIGINAL PAPER

Andreas Lüttge · Edward W. Bolton · Danny M. Rye

A kinetic model of metamorphism: an application to siliceous dolomites

Received: 7 May 2003 / Accepted: 16 September 2003 / Published online: 16 October 2003

Abstract We use a kinetic model of a metamorphic system to study the effect of competing rates of reaction, fluid injection, and heating on the evolution of the "reaction pathway" in temperature/composition space at constant pressure. We show that for rocks in contact with mixed volatile (e.g., CO_2-H_2O) fluids the reaction path may be quite different from what is expected from equilibrium-based petrologic models. Equilibrium-based models, used to understand the development of rock systems undergoing mineral reactions during a metamorphic event, rely on the Gibbs' phase rule and only consider stable phases. For constant pressure, the temperature-composition paths follow univariant curves and significant reactions may occur at invariant points. By contrast, the more general kinetic treatment is not constrained by equilibrium, although with the proper competing rates equilibrium is a possible endmember of the kinetic approach. The deviation from equilibrium depends on the competing rates of reaction, heating, and fluid injection. A key element required by the kinetic approach is the inclusion of metastable reactions in the formulation, whereas such reactions are irrelevant for equilibrium-based models. Metastable reactions are often involved in a complex interplay with common prograde stable metamorphic reactions. We present model results for the well-studied CaO-MgO-SiO_2-CO_2-H_2O (CMS) system to show how the system evolves under kinetic control. Our simulations and discussion focus on the behavior of the CMS system under a number of closed and open system conditions. Special attention is paid to closed system behavior in the vicinity of the (first) isobaric invariant point (with Dol, Qtz, Tlc, Cal, and Tr). Also, for open systems with massive fluid infiltration we consider heating rates varying from contact to regional metamorphic conditions. For some geologically reasonable rates of reactions, heating, and fluid injection, our results demonstrate that equilibrium conditions may be significantly overstepped in metamorphic systems. We used overall mineral reactions in this model with rates based on experimental results. Future models could rely on more fundamental dissolution and precipitation reactions. Such an extension would require additional kinetic rate data, as well as mineral solubilities in mixed volatile fluids.

Editorial responsibility: J. Hoefs

A. Lüttge (✉) · E. W. Bolton · D. M. Rye
Department of Geology and Geophysics, Yale University,
New Haven, CT 06520-8109, USA
E-mail: aluttge@rice.edu

A. Lüttge
Department of Earth Science, Rice University,
Houston, TX 77251-1892, USA

Introduction

The application of equilibrium thermodynamics to heterogeneous systems was formulated by Gibbs (1878). Subsequent discussions of open and closed geochemical systems provided a framework for petrologists to use thermodynamics to interpret rock systems (Eskola 1915; Miyashiro 1961; Korzhinskii 1950, 1957, 1966, 1967; Thompson 1955, 1959, 1970; Weill and Fyfe 1964, 1967; Rice 1977a, 1977b).

Greenwood (1975) and later Rice (1977b) and Rice and Ferry (1982) developed an equilibrium thermodynamic treatment of internally buffered mixed-volatile-rock-systems undergoing metamorphism. Extensions of this work have lead to the presently accepted equilibrium-based understanding of contact metamorphism as driven by fluid infiltration coupled with chemical reactions in rocks (e.g., Ferry 1991; Spear 1995, and references therein, see also Walther and Orville 1982; Ferry and Dipple 1991).

Experimental work and theoretical considerations have led to the construction of petrogenetic grids (*P*-*T* or *T*-*X* diagrams for constant pressure, e.g., Fig. 1, and Table 1: here we use symbols *P*: pressure, *T*: temperature, and *X*: composition, usually the mole fraction of CO_2 in the H_2O–CO_2 supercritical mixture) that are the

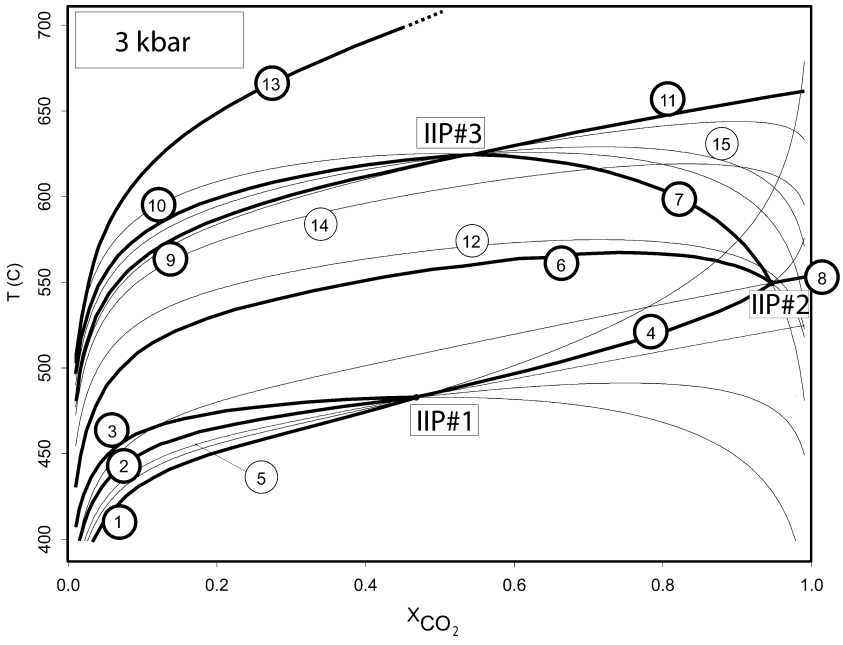

Fig 1 Isobaric-T- X_{CO2} diagram showing 15 equilibrium curves (with their metastable extensions) of reactions occurring in the system CaO-MgO-SiO_2-CO_2-H_2O, at a pressure of 3 kbar. The mineral reactions are numbered as in Table 1. *Bold circles* near *bold curves* indicate stable reactions, while *thin circles* by *thin curves* indicate metastable reactions. Three isobaric invariant points are indicated

Table 1 Reactions in the system CaO-SiO_2-MgO-H_2O-CO_2. In the calculations, the stoichiometric coefficients were modified from these values by dividing each reaction by the factor multiplying CO_2in the reactions shown below (e.g., reaction 1 was divided through by 3). Formulas assumed are Dol: $CaMg(CO_3)_2$; Qtz: SiO_2; Cal: $CaCO_3$; Tlc: $Mg_3[Si_4O_{10}(OH)_2]$; Tr: $Ca_2Mg_5[Si_8O_{22}(OH)_2]$; Di: $CaMg[Si_2O_6]$; Fo: $Mg_2[SiO_4]$; Wo: $CaSiO_3$

(1)	3 dolomite + 4 quartz + 1 H_2O	⇔	1 talc + 3 calcite + 3 CO_2
(2)	5 talc + 6 calcite + 4 quartz	⇔	3 tremolite + 6 CO_2 + 2 H_2O
(3)	2 talc + 3 calcite	⇔	1 tremolite + 1 dolomite + 1 CO_2 + 1 H_2O
(4)	5 dolomite + 8 quartz + 1 H_2O	⇔	1 tremolite + 3 calcite + 7 CO_2
(5)	1 talc + 2 dolomite + 4 quartz	⇔	1 tremolite + 4 CO_2(metastable reaction)
(6)	1 tremolite + 3 calcite + 2 quartz	⇔	5 diopside + 1 H_2O + 3 CO_2
(7)	1 tremolite + 3 calcite	⇔	4 diopside + 1 dolomite + 1 CO_2 + 1 H_2O
(8)	1 dolomite + 2 quartz	⇔	1 diopside + 2 CO_2
(9)	1 tremolite + 11 dolomite	⇔	8 forsterite + 13 calcite + 9 CO_2 + 1 H_2O
(10)	3 tremolite + 5 calcite	⇔	2 forsterite + 11 diopside + 5 CO_2 + 3 H_2O
(11)	1 diopside + 3 dolomite	⇔	2 forsterite + 4 calcite + 2 CO_2
(12)	13 talc + 10 dolomite	⇔	5 tremolite + 12 forsterite + 20 CO_2 + 8 H_2O
(13)	1 quartz + 1 calcite	⇔	1 wollastonite + 1 CO_2
(14)	1 talc + 5 dolomite	⇔	4 forsterite + 5 calcite + 5 CO_2 + 1 H_2O
(15)	4 tremolite + 5 dolomite	⇔	6 forsterite + 13 diopside + 10 CO_2 + 4 H_2O

typical framework for discussion of the development of metamorphic rocks. A cornerstone in the interpretation of many metamorphic rocks is the development of a particular system "at" the isobaric invariant points or singular points of the systems (e.g., Greenwood 1975; Rice and Ferry 1982; Rice 1977b; Spear 1995). The invariant and singular points are of particular interest if the fluid composition is internally buffered (Greenwood 1975; Rice and Ferry 1982). The importance of invariant or singular points is clear under the assumption that the system is closed to fluid flow. In the equilibrium model, small amounts of reaction along univariant curves drive the system to the invariant or singular points, where most of the conversion of one mineral assemblage to another occurs.

Away from equilibrium any of the overall reactions whose univariant curves intersect at the isobaric invariant point can proceed, if the right reactants and/or products are present. However, thermodynamic equilibrium is not possible while heat or mass, in the form of nonequilibrium fluid, is "pumped" into or out of a system. As a result, the invariant point is only meaningful as an attractor. The degree of attraction depends strongly on external influences, i.e., heating rates, fluid flow, composition, and reaction rates. For example, if the heat input stops at some later time, the system will evolve from its initial non-equilibrium state and approach the (isobaric) invariant point (as will be shown below).

For open systems at a fixed pressure, fluid composition is typically considered to be determined by a balance of the infiltrating fluid and reaction produced fluid. The resultant fluid has a temperature and composition on an equilibrium curve (e.g., Hewitt 1973; Roselle et al. 1999). The assumption of fluid buffering at, or near, equilibrium leads to the ability to calculate the amount of fluid added to the system.

Whereas many petrographic observations of the sequence of mineral assemblages in nature are consistent with equilibrium phase diagrams, an increasing number

of studies have pointed out the relevance of kinetic control (e.g., Steefel and Lasaga 1990, 1992, 1994; Steefel and Van Cappellen 1990; Balashov and Yardley 1998; Connolly 1997; Lattanzi et al. 1980; Lasaga 1998; Lasaga and Rye 1993; Lasaga et al. 2000, 2001; Lüttge et al. 1997a, 1997b, 1998; Bolton et al. 1999, 2003; Baxter and DePaolo 2000, 2002a, 2002b). In general, the consistency of petrographic observations with equilibrium phase diagrams is a necessary, but not sufficient condition, to prove that equilibrium was achieved. Increasingly, studies have demonstrated that in cases where the phase assemblage is consistent with equilibrium, the phases present do not require that equilibrium occurred. In several studies, petrographic observations, petrogenetic interpretation, and/or stable-isotope data are not in agreement with an equilibrium model (Lattanzi et al. 1980; Ridley and Thompson 1986; Kerrick 1990; Ernst and Banno 1991; Lasaga and Rye 1993; Manning et al. 1993; van Haren et al. 1996; Rubie 1998; Giorgetti et al. 2000; Baxter and DePaolo 2000, 2002a, 2002b; Lasaga et al. 2001). It should be noted that field observations of a sequence of mineral occurrences can often be explained by equilibrium models, but kinetic models can give rise to the same sequence, even for systems that evolved under far from equilibrium conditions (Lasaga and Rye 1993).

For example, each five-phase mineral assemblage, expected to occur only at isobaric invariant conditions in an equilibrium model (e.g., dolomite + quartz + talc + calcite + tremolite), can be obtained if at least two univariant curves are overstepped (see Figs. 2 and 3, and Lasaga et al. 2000, 2001). In the future, petrographic criteria must be developed that use the detailed mineral texture variations (cf. Yardley 1993, p. 161) in nature to distinguish between equilibrium and non-equilibrium scenarios in metamorphic rocks.

Lasaga and Rye (1993) showed that metamorphism of rocks needs to be understood as the interaction of heat flow, fluid flow, and reaction rates. And again, in Lasaga et al. (2000) it is shown that "*the correct assumption that the rates of many of the physical processes are fast enough to adapt, at least in most cases, to the inputs from geologic processes*" does not automatically lead to thermodynamic equilibrium. This statement can be tested with a relatively simple model for a large variety of geologic parameters, i.e., heating rates, fluid flow rates, and reaction rates (Lasaga et al. 2000, 2001).

The assumption of equilibrium for a reacting system is problematical because *processes* cannot be understood in an equilibrium model. In effect, all processes have a path but equilibrium is independent of path. If one were interested in just predicting the stability of minerals in nature and the sequence in which they would occur, both equilibrium thermodynamics and kinetics would give about the same answer and there would be little disagreement. However, geologists are interested ultimately in the actual processes occurring in the earth; to quantify these processes requires a model that is inherently kinetic. Again, the attainment of equilibrium is always a possibility in a kinetic model but the converse is not true. It could be that all metamorphic processes involving mineral reactions occur very close to equilibrium. The proof of that statement, however, will only come from a

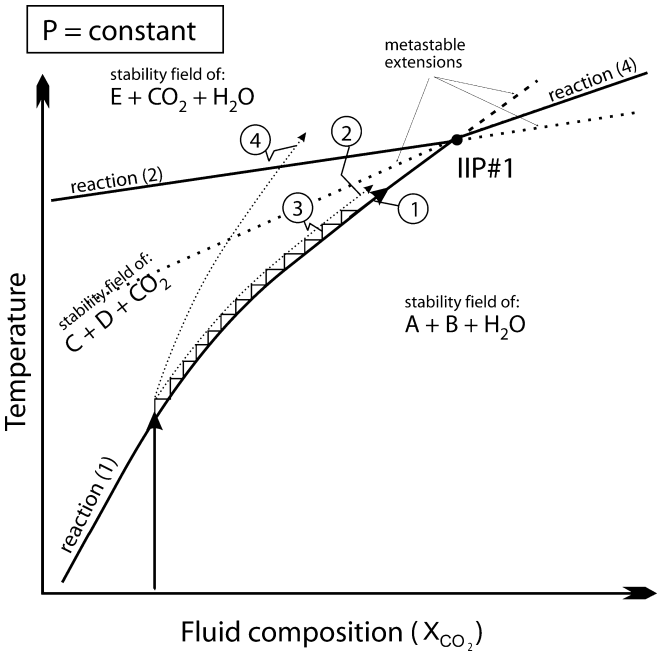

Fig 2 Sketch that shows different pathways along a univariant equilibrium curve. Path *1*: evolution of the system following Greenwood's (1975) and Rice and Ferry's (1982) approach for a "closed" system; path *2* near equilibrium path according to our model; path *3* "stair-like" development, often used in discussions; path *4* example of a "far"-from-equilibrium path leading to a high T-overstep. See also Fig. 3

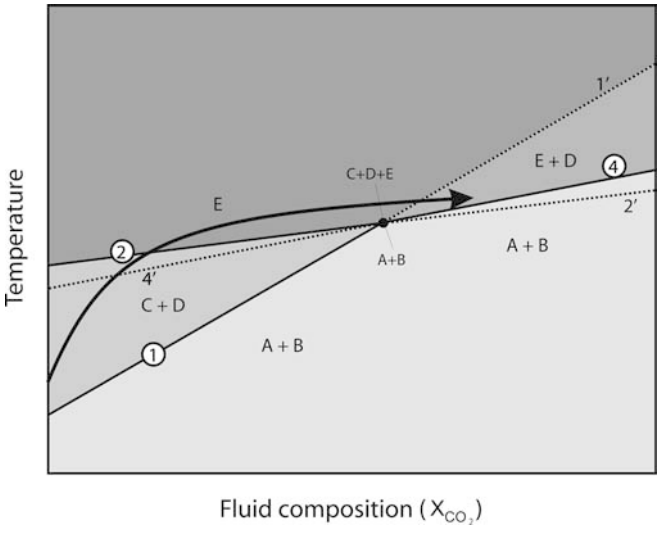

Fig 3 Sketch that schematically shows the stable mineral phases (*A*, *B*, *C*, *D*, and *E*) and three equilibrium curves [reactions (1), (2), (4)] with their metastable extensions (*dotted lines*) in the vicinity of an (isobaric) invariant point. The overstep of two univariant curves can lead to the mineral assemblage A + B + C + D + E. This assemblage is identical with the equilibrium assemblage at the isobaric invariant point; see text for detailed discussion

careful kinetic analysis of the kinetic rate laws and rates of change in the important intensive variables (e.g., P, T, or X_{CO2} mole fraction of CO_2) that characterize the system.

Thermodynamics was originally developed in order to understand equilibrium relationships between heterogeneous substances (Gibbs 1878). In the context of geological systems, self-consistent thermodynamic databases have been developed that unify experimental results from petrologic studies of equilibrium phase boundaries. These databases allow for the calculation of thermodynamic functions (e.g., entropy, enthalpy, Gibbs free energy, etc.) for minerals and mixed volatiles relative to reference states. The free energy change for mineral/fluid reactions can then be calculated even for conditions that are NOT in equilibrium (e.g., for mineral assemblages and P-T-X conditions not in their stability fields), as the thermodynamic functions retain their meaning even when the system is not in equilibrium. Given the simple assumption that the rates of reaction depend on the deviation from equilibrium (as measured by the Gibbs free energy of the overall reaction), and by use of experimental measurements of rates of metamorphic reactions as a function of this deviation, it is possible to combine kinetics with thermodynamic data bases for a kinetic model. We use overall reactions in this model, with rates based on experiments on representative metamorphic reactions. To proceed beyond the approach of using overall reactions, more kinetic data is needed for relevant dissolution and precipitation reactions. There is also a need for comprehensive data and models for solubilities of minerals in supercritical CO_2-H_2O mixtures, as well as the influence of salts in such systems. When such data become available, our modeling effort can move beyond the simplified approach that makes use of overall reactions.

Because reactions in open systems can be overstepped, metastable reactions are important in a kinetic treatment. Within an equilibrium thermodynamic treatment, metastable reactions play no role because no metastable phases are present. Therefore, the equilibrium thermodynamic approach ignores metastable phases and metastable reactions. Likewise, metastable extensions have been often ignored in petrological phase diagrams. On the other hand, metastability is often encountered when kinetically controlled reactions are considered. Many reactions can only take place because of the role of metastable intermediates (e.g., Lasaga 1998). For example, many mineral reactions require the mediation of metastable mineral phases, e.g., the formation of tremolite (Steefel and Van Cappellen 1990).

The occurrence and the kinetics of metastable reactions in metamorphic conditions have been well studied in a number of experimental studies (e.g., Lüttge and Metz 1991, 1993; Lüttge et al. 1998; Jordan et al. 1992). In some cases, the equilibrium conditions of such metastable reactions were also experimentally determined (Metz, personal communication). There is no reason to assume that metastable reactions would occur in the laboratories but not in nature. The same rules of physical chemistry apply to metastable reactions as to stable reactions, and one cannot ignore metastable extensions in any dynamic model or description of metamorphic processes in which overstepping may result in conditions that allow a metastable reaction to proceed. If the equilibrium extension of a metastable reaction is overstepped and all the appropriate reactants are present, thermodynamics dictate that the metastable reaction will proceed to operate in the forward direction.

In this paper, we contrast the equilibrium-based approach with results that illustrate the influence of kinetic control in metamorphic systems. Of course, equilibrium is always an endmember of the more general kinetic approach, but we will show that under kinetic control, systems may evolve also along unexpected pathways.

To make these comparisons, we have chosen a five-component system (CaO-MgO-SiO_2-CO_2-H_2O), i.e., the CMS-system in the presence of a mixed CO_2-H_2O fluid, as a simplified but sufficient example to explore the implications of kinetic control of metamorphic reactions. This system has been very well studied theoretically, experimentally, and also in nature, (e.g., Berman 1988; Gottschalk 1997; Metz 1967, 1970; Metz and Puhan 1970; Dachs and Metz 1988; Heinrich et al. 1986, 1989; Kridlebaugh 1971, 1973; Käse and Metz 1980; Lüttge and Metz 1991, 1993; Lüttge et al. 1998; Tanner et al. 1985; Walther 1996; Winkler and Lüttge 1999; Skippen and Trommsdorff 1975; Trommsdorff 1972; Heuss-Aßbichler and Masch 1991; Masch and Heuss-Aßbichler 1991, Roselle et al. 1999). A list of important earlier papers that applied the theory of mixed-volatile equilibria to metamorphic rocks is given by Tracy et al. (1983). For an excellent review of contact metamorphism of siliceous carbonates, which also addresses directions of fluid flow, see Ferry et al. (2002).

As mentioned above, we have included some metastable reactions in our formulation, as required for a kinetic model. To make some of these concepts more concrete, we offer a brief discussion about the reactions included around the first isobaric invariant point (IIP#1 with stable phases: Dol-Qtz-Tlc-Cal-Tr). We have included ALL univariant reactions involving these phases (yet ignoring solid solution). Each of these five reactions (Table 1) that meet at IIP#1 involve four minerals (each of the reactions has one of the five absent). We normalized all the rates to refer to reactions with one mole of CO_2 produced. Between the univariant curves that meet at IIP#1, the phase rule based on equilibrium would allow at most three minerals in contact with the fluid. In a kinetic model, curves may be overstepped, so four or all five of these minerals could coexist, with one or more reactions running simultaneously. In addition, some of the reactions could "run backwards", e.g., if X_{CO2} is smaller than that of the IIP#1, and if reactions 1 and 4 are overstepped, Tr, Cal, and Tlc would be produced from Dol-Qtz, which allows reactions 2, 3, and 5 to run in reverse. The instantaneous amount of each mineral forming or being consumed depends on the

kinetic rates of each reaction running forward or backward, which in turn depends on evolving mineral surface areas in contact with the fluid. The stoichiometry of minerals being produced or destroyed during simultaneous reactions may not correspond to any one reaction, but the combinations of several reactions, each with their own evolving rate. We have also tested the model without including reaction 5. The results of this test were only slightly different from including all five reactions near that invariant point. Even so, we feel more the complete set of reactions is more consistent than arbitrarily omitting one.

In order to apply kinetic models we need to have rates of reactions and processes. Except for one case with no heat input, we consider heating rates from 10^{-3} to 10^{-1} °C/year. Aside from cases without fluid injection, we considered input pore velocities injected into the system ranging from 10^{-4} to 10^{-1} m/year. Although this is a small sampling of rates for heating and fluid injection relevant to contact metamorphism, we felt this to be a reasonable range to consider for this initial application of a kinetic model. More realism will be included in our future two-dimensional models, which combine kinetic control of reactions along with flow and reaction around a pluton. This should provide a useful extension of the existing models of heat and fluid flow around plutons (see Cui et al. 2002, and references therein).

Overall mineral reactions actually occur via dissolution and precipitation of individual minerals (e.g., Heinrich et al. 1986, 1989; Lasaga 1986, 1998; Lüttge and Metz 1991, 1993; Lüttge et al. 1998; Matthews and Goldsmith 1984; Milke and Metz 2002; Schramke et al. 1987; Tanner et al. 1985; Winkler and Lüttge 1999). Such reactions are dependent on the kinetics of dissolution and growth of the individual mineral phases. The available experimental kinetic data on the overall reactions reflect the rates of these underlying individual reactions. Although our current model has a simple linear dependence of the reaction rates upon the deviation from equilibrium, some experimental studies of the variation in the rates of mineral-fluid reactions (e.g., Cama et al. 2000; Burch et al. 1993; Nagy and Lasaga 1992; Taylor et al. 2000) have shown the presence of very non-linear rates as a function of deviation from equilibrium. Similar nonlinear rates are likely for overall mineral reactions. Therefore, the linear extrapolation of such rate data, to conditions very close to equilibrium, could strongly overestimate the rate. Consequently, estimates of overstepping based on the linear extrapolation we used are likely to underestimate the actual deviation from equilibrium (e.g., Walther and Wood 1984; Lasaga and Rye 1993; Lasaga et al. 2000, 2001). As more experiments are performed that extract kinetic rates of dissolution and precipitation, we could move beyond the present simplified approach that uses overall reactions. As mentioned above, additional solubility data is also necessary in these mixed volatile fluids.

Model and results

Model description

We have developed a computer model to study the implications of reaction kinetics on the possible *T-P-X*-development of rocks undergoing metamorphism. This model uses a thermodynamic database to calculate free energy changes during reactions. It also includes finite reaction rates dependent on deviations from equilibrium, as well as injection of fluid and heat into the system. We have explored the behavior of an idealized siliceous dolomite (CMS-system: CaO-MgO-SiO_2-CO_2-H_2O) for a wide range of geologic parameters. We present some of the key results that illustrate points made in the introduction.

Our modeling of this system is simplified in many ways compared to natural rocks, yet it should capture important aspects of the dynamics. Many of the same simplifications made here are also inherent in traditional equilibrium based models. Simplifications include the assumption of pure CO_2-H_2O fluids (the other elements [Ca, Mg, and Si] exchange only locally, i.e., either solubility of other elements is constant, or their transport is limited). Future models that move beyond this simplification will require more laboratory measurements of solubility in supercritical CO_2-H_2O mixtures. Our model also ignores solid solution (e.g., dolomite and calcite are considered as their pure endmembers). Additional details of the calculations, as well as examples of flow and

►

Fig 4 Model results for the development of a reaction path around the first isobaric invariant point (CMS system at 3 kbar) in the case of no heating and no fluid injection; initial fluid porosity fraction 4×10^{-3}; **a** *T-X* evolution of the system. Initial condition for *T* and *X* are indicated by the *square*. See text for initial mineral composition. *Circles* of increasing radii with time are placed along the path, separated by equal times, with *T-X* evolution changing more slowly near the invariant point. Reaction numbers are as in Table 1; **b** temperature evolution as a function of time. The *dashed line* is the temperature of the invariant point; **c** X_{CO2} evolution as a function of time The *dashed line* is the composition of the invariant point; **d** rates of ongoing reactions (*positive values* for forward reactions, *negative values* for backward reactions, both in mol/m^3_{bulk}/year); **e** development of modal fractions of the minerals and the porosity with time (In this figure, and others to follow: *Cal* calcite, *Di* diopside, *Dol* dolomite, *Fo* forsterite, *Qtz* quartz, *Tlc* talc, *Tr* tremolite, *Wo* wollastonite); **f** total production of H_2O and CO_2 as a function of time. *Negative values* indicate consumption. H_2O: (*solid*), CO_2: (*dashed*); **g** variation of rates of fluid production (CO_2-produced vs. H_2O-produced, both in units of [moles/m^3_{fluid}/year]); **h** CO_2/H_2O ratio extant in the box (*long dashed line*); ratio being produced by reactions (*solid line*, clipped at 1.475); ratio of the isobaric invariant point (*short dashed*). The apparent divergence of the fluid production ratio is only indicative of vanishing H_2O production. Note that the ratio of fluid produced does not correspond to the invariant point composition; **i** in order to maintain constant pressure, fluid must be extracted from the system: "out": mass flux out of the system divided by Δx_{sys} (*long-dashed line*); "in": mass flux into the system divided by Δx_{sys} (*solid line*, at zero for this case); fluid production rate by reaction within the 1 m^3 (*short-dashed*); see text for detailed discussion

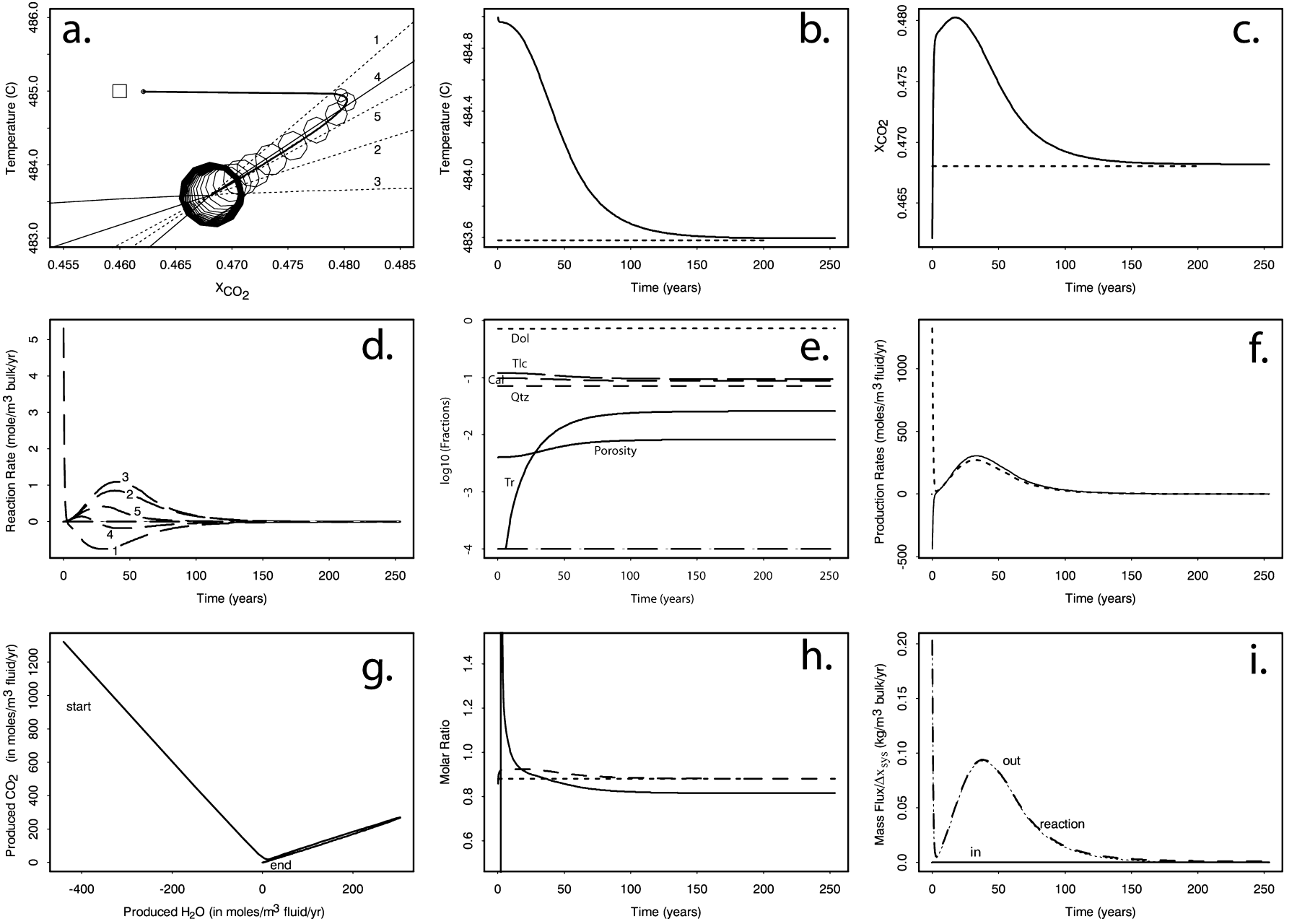
a.
Temperature (C)
X_{CO_2}
1
4
5
2
3
b.
Temperature (C)
Time (years)
c.
X_{CO_2}
Time (years)
d.
Reaction Rate (mole/m3 bulk/yr)
Time (years)
e.
log10 (Fractions)
Dol
Tlc
Cal
Qtz
Porosity
Tr
Time (years)
f.
Production Rates (moles/m3 fluid/yr)
Time (years)
g.
Produced CO_2 (in moles/m3 fluid/yr)
start
end
Produced H_2O (in moles/m3 fluid/yr)
h.
Molar Ratio
Time (years)
i.
Mass Flux/Δx_{sys} (kg/m3 bulk/yr)
out
reaction
in
Time (years)

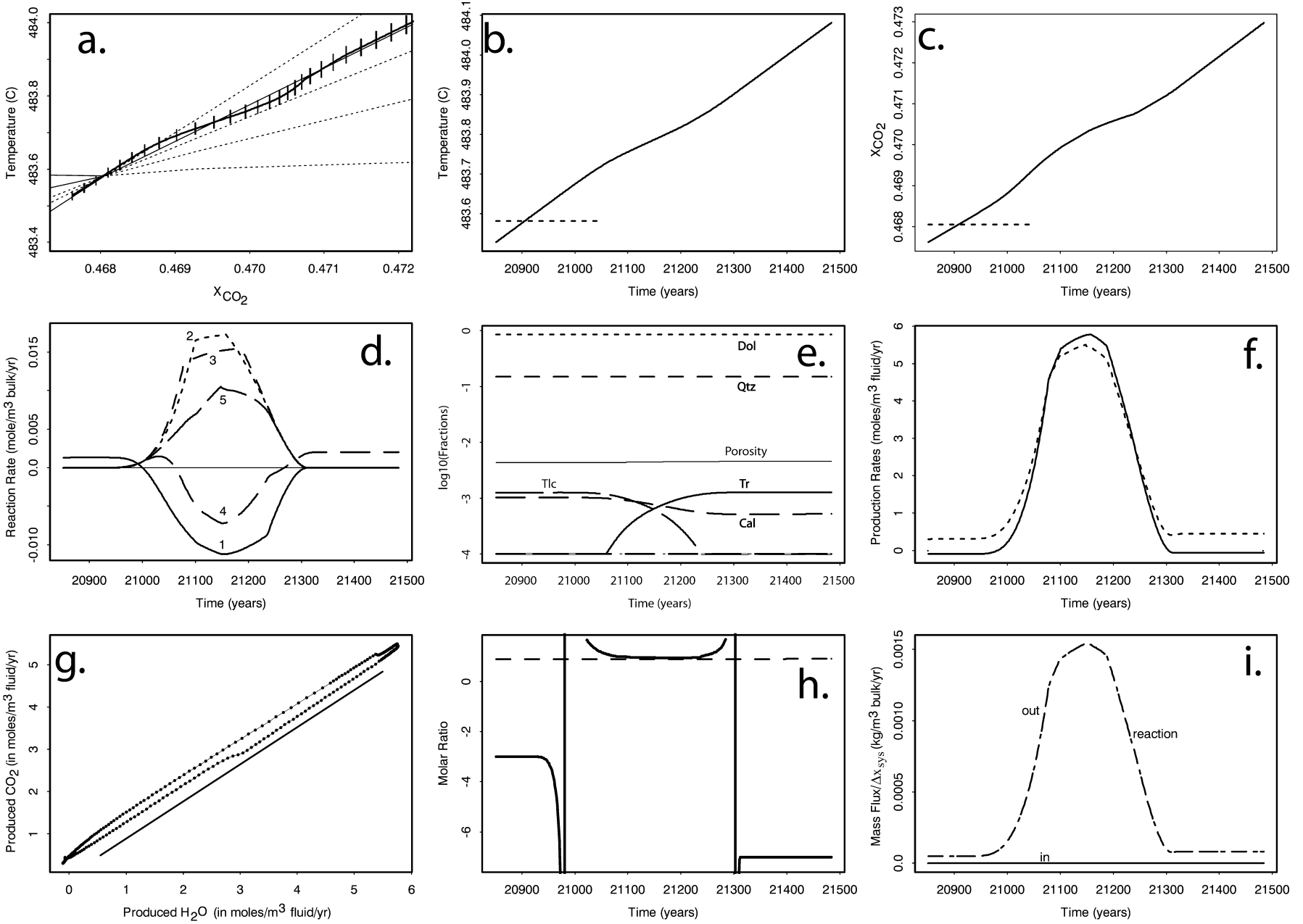
a.
Temperature (C)
484.0
483.8
483.6
483.4
0.468
0.469
0.470
0.471
0.472
X_{CO_2}
b.
Temperature (C)
484.1
484.0
483.9
483.8
483.7
483.6
20900
21000
21100
21200
21300
21400
21500
Time (years)
c.
X_{CO_2}
0.473
0.472
0.471
0.470
0.469
0.468
20900
21000
21100
21200
21300
21400
21500
Time (years)
d.
Reaction Rate (mole/m3 bulk/yr)
0.015
0.005
0.0
-0.010
2
3
5
4
1
20900
21000
21100
21200
21300
21400
21500
Time (years)
e.
log10(Fractions)
0
-1
-2
-3
-4
Dol
Qtz
Porosity
Tlc
Tr
Cal
20900
21000
21100
21200
21300
21400
21500
Time (years)
f.
Production Rates (moles/m3 fluid/yr)
6
5
4
3
2
1
0
20900
21000
21100
21200
21300
21400
21500
Time (years)
g.
Produced CO_2 (in moles/m3 fluid/yr)
5
4
3
2
1
0
1
2
3
4
5
6
Produced H_2O (in moles/m3 fluid/yr)
h.
Molar Ratio
0
-2
-4
-6
20900
21000
21100
21200
21300
21400
21500
Time (years)
i.
Mass Flux/Δx_{sys} (kg/m3 bulk/yr)
0.0015
0.0010
0.0005
0.0
out
reaction
in
20900
21000
21100
21200
21300
21400
21500
Time (years)

◀

Fig 5 Simulation with external heating: heat is injected at a "rate equivalent" of 1 °C/10^3 year (see text), while no fluid is injected; **a**–**i** is a summary of results obtained around the isobaric invariant point (these details are for a limited time span from a longer simulation). Initial volume fractions (compared to the bulk volume) of dolomite and quartz for all the remaining cases were specified as 0.846 and 0.15, respectively, making the initial fluid porosity fraction 4×10^{-3}; for detailed discussion, see text and compare Fig. 4. In part **a**, *tick marks* are made for equal time intervals: note there is no pause at the isobaric invariant point. In part **g**, *dots* are placed equally spaced in time. Below the *dotted* evolution of the system is a *line* indicating the ratio of the invariant point

reaction of this system in the context of contact metamorphism in two dimensions, are in preparation (Bolton et al. 2003), where the fluid flow in the domain is a function of buoyancy and reactive production of volatiles.

As discussed above, Fig. 1 shows a T-X_{CO2} diagram of the CMS system for a constant pressure of 3 kbar (300 MPa). Curves representing equilibrium ($\Delta G = 0$) for 15 overall mineral reactions (see also Table 1) are presented with their metastable extensions in this diagram. The Gibbs free energies throughout the grid were calculated using the self-consistent data set of Berman (1988). Such a database allows for the calculation of free energy changes of reactions even far from equilibrium. For simplicity, we ignored the minor changes in mineral density, which can accompany changes in pressure and temperature (this effect makes a difference of typically less than 2 °C on the location of the equilibrium curves). We used the fugacity and equation of state estimates for supercritical H_2O-CO_2 mixtures of Jacobs and Kerrick (1981) and Kerrick and Jacobs (1981). Several of our case studies focus on various metamorphic conditions near the region of the first invariant point (with phases Dol, Qtz, Tlc, Cal, and Tr possibly present), which for this pressure is located near $X_{CO2}\cong0.47$ and $T\cong484$ °C.

Each overall mineral reaction has a unique reaction rate law of the form:

$$J_i = k_{0:i}\frac{A_{m*(i)}}{V_B\left|v^i_{s:m*}\right|}\exp\left(-\frac{E^i_a}{RT}\right)f(\Delta G_i), \qquad (1)$$

where, J_i is the rate of the i^{th} reaction (to the right as written in Table 1, in mol/((m^3 bulk) sec), [except we first divide all coefficients by the stoichiometric factor multiplying CO_2, this has the effect of normalizing the rate of each reaction to "one mole of CO_2 produced"]). The prefactor $k_{0:i}$ is an overall rate constant for that reaction (in mol m^{-2} sec^{-1} (J mol^{-1}) $^{-1}$), which may in general vary with pH, X_{CO2}, and temperature, although we used constant $k_{0:i}$ values (still, reaction rates depend on the other factors in Eq. (1)). The variable, $A_{m*(i)}$ is the surface area of the rate limiting mineral m* (see below) in contact with the fluid contained in a reference bulk volume V_B. Also, $|v^i_{s:m*}|$ is the absolute value of the stoichiometric coefficient of the rate limiting mineral for reaction i, E^i_a is the apparent activation energy for the overall reaction (J/mole), R is the gas constant (J/mole/deg), T is the absolute temperature, and $f(\Delta G_i)$ is a function of the change of the Gibbs free energy for the overall reaction (normalized to "one mole of CO_2 produced"). Note that there is always a dependence of reaction rate on ΔG of the overall reaction. In our model, for $f(\Delta G_i)$ we used ΔG itself. This results in reaction rates linearly dependent on the deviation from equilibrium. This choice contributes to how experimental kinetic rates become translated into specific values of the prefactor $k_{0:i}$. If the minerals, which would be consumed when the reaction proceeds, are not present in quantities above some small threshold, then the reaction rate is set to zero. In fact, all reactions involving each mineral must be summed in order to assess whether the net effect would consume the mineral present in low levels. Otherwise, spurious oscillations can be created with a mineral growing by one reaction during one time step, only to be consumed by another reaction in the next time step.

Each reaction has its own stoichiometry and each mineral has an evolving surface area. As surface areas change, the mineral that limits the rate of a given overall reaction can switch from one mineral to another. In our model, the mineral, m*, which limits the rate of reaction i during a given time step, is the m that minimizes $A_m/|v^i_{s:m}|$ for all m. This effectively weighs each mineral equally. This restriction could be relaxed in future models when more quantitative kinetic data is available. Note that we assume that fluid is always present.

We used rate data from Schramke et al. (1987) with 20 kcal/mole apparent activation energies (83,630 J/mol) with each reaction in Table 1 normalized to one mole of CO_2 produced. This approach gives $k_0 = 2.6\times10^{-7}$ [mol m^{-2} sec^{-1} (J mol^{-1}) $^{-1}$], which we used for each of the reactions. Our use of such experimental rates is conservative (i.e., fast), in that, Baxter and DePaolo (2000, 2002a, 2002b) have reported reaction rates from a natural system that are from one to even several orders of magnitude slower than the experimental rates used in this study. The choice we make here is similar to the 4×10^{-15} mol cm^{-2} s^{-1} K^{-1} rate found in Lasaga et al. (2000), where the overstep was expressed in units of temperature rather than J×$mole^{-1}$.

In each of our simulations the fluid porosity fraction of 4×10^{-3} was set for the initial system (the porosity φ is a ratio of the fluid volume to the bulk volume: V_f / V_B). A minute quantity of each mineral was imposed as "seed crystals" to avoid dealing with nucleation problems. Future models must deal with nucleation barriers in a self-consistent way; a complication we avoid for the present study.

Grain centers of each mineral type were assumed to be separated by $L = 0.4$ mm in a cubic grid for all simulations of this study. This spacing yields a nucleation density of $(1/64)\times10^{12}$ grains/m^3 bulk for each mineral type. The grains themselves were assumed to be cubes (the cube edge lengths are $d_m = L\,(\varphi_m)^{1/3}$ where φ_m is the volume of mineral m per bulk volume). The surfaces of the grains were assumed to always be in contact with the

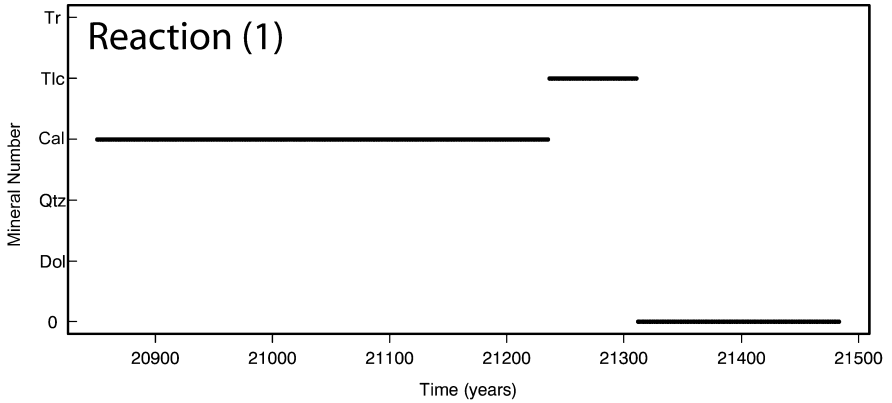
Reaction (1)
Mineral Number
Tr
Tlc
Cal
Qtz
Dol
0
20900
21000
21100
21200
21300
21400
21500
Time (years)

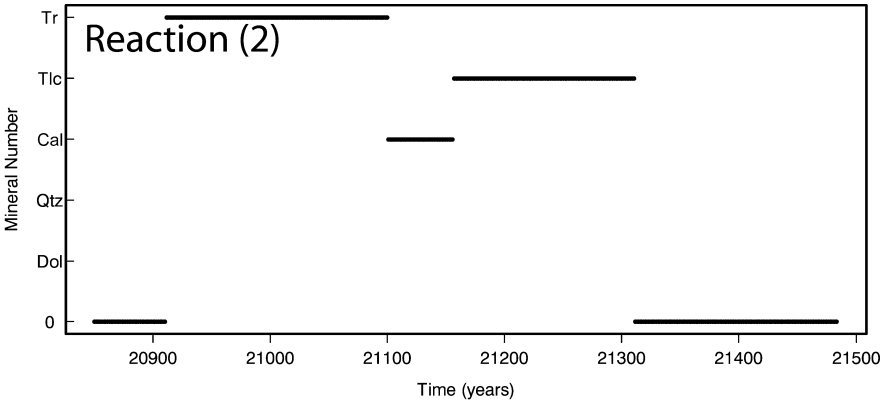
Reaction (2)
Mineral Number
Tr
Tlc
Cal
Qtz
Dol
0
20900
21000
21100
21200
21300
21400
21500
Time (years)

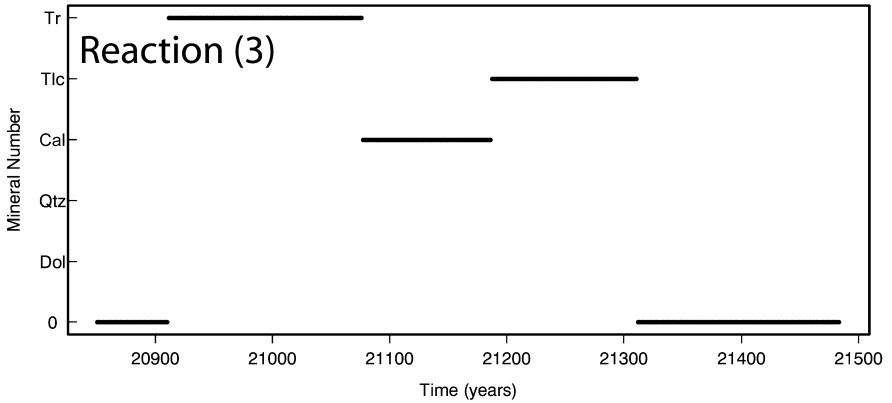
Reaction (3)
Mineral Number
Tr
Tlc
Cal
Qtz
Dol
0
20900
21000
21100
21200
21300
21400
21500
Time (years)

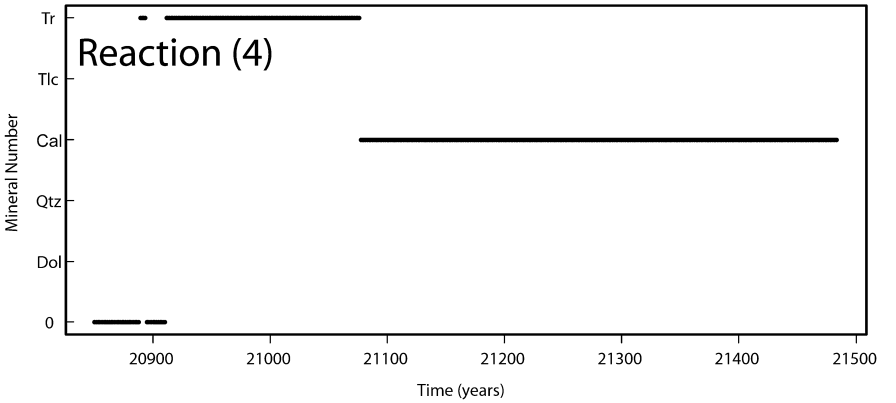
Reaction (4)
Mineral Number
Tr
Tlc
Cal
Qtz
Dol
0
20900
21000
21100
21200
21300
21400
21500
Time (years)

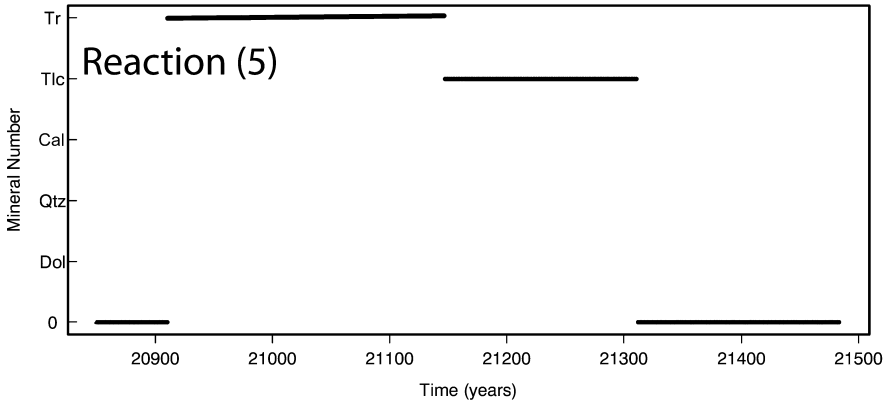
Reaction (5)
Mineral Number
Tr
Tlc
Cal
Qtz
Dol
0
20900
21000
21100
21200
21300
21400
21500
Time (years)

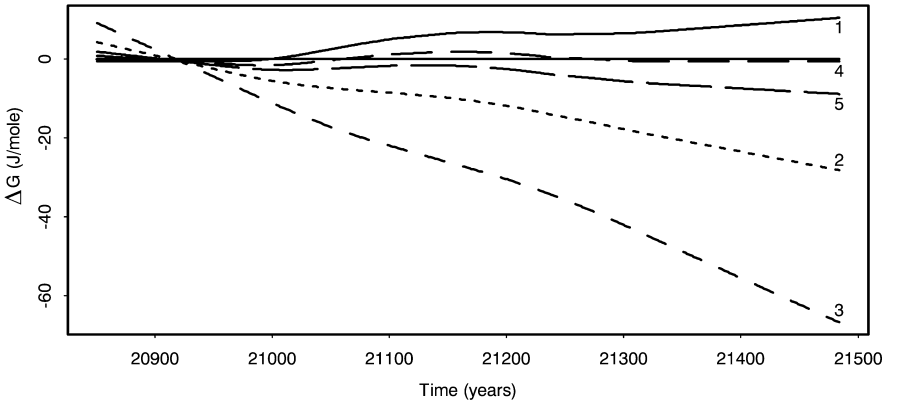
ΔG (J/mole)
0
-20
-40
-60
1
4
5
2
3
20900
21000
21100
21200
21300
21400
21500
Time (years)

◄

Fig 6 Shown are the minerals that limit the rate of each of the five reactions for the time period when the system passes near the isobaric invariant point; times of no reaction are indicated with a "*zero*". The lower right part of the figure shows the evolution of ΔG_k for the five reactions. By comparing this figure to Fig. 5d, one can deduce the critical importance of mineral surface areas in limiting the reaction rates; see text for detailed discussion

metamorphic fluid. This approach is conservative in the sense that overstepping of equilibrium curves is discouraged by the large exposed surface area of each grain (compared to a grain model where the fluid is in contact with tubes at boundaries of three or more grains). The textural issues of impingement and occlusion were ignored. Grain sizes evolved (as well as the porosity) according to the rates of each reaction, the stoichiometric coefficients, the mineral areas exposed, and the molar volumes of the respective mineral.

The fluid composition evolves via conservation of mass for the system, including the possibility of consumption or production of H_2O and CO_2, as well as fluid injection and withdrawal from the system. For the purposes of this study, we chose the system to be a cube with side dimensions of 1 m (cf. Lasaga et al. 2000). We calculate both the evolution of X_{CO2}, and the total moles of H_2O and CO_2. Fluid could be injected into the system at specified molar rates and compositions (X_{CO2}). When fluid was produced by reaction, it mixed with extant fluid. In any case, enough fluid was extracted from the system in order to maintain the fluid pressure at 3 kbar at the end of each time step. We also compute the evolution of temperature for the system (using solid densities and specific heats yielding 3.4×10^6 J m^{-3} K^{-1}). Enthalpies of reaction caused heating or cooling of the system. In addition, some cases included specified rates of heat injection (rather than imposed temperature changes). This method allows for the possibility that heat added to the system could in turn be consumed by endothermic reactions, without appreciable change in temperature. Indeed, such behavior was observed during some time periods of the simulations.

Model results

Cases without fluid injection

Our first illustration of the time-dependent behavior of the CMS system is for a case where no heat or mass is injected into the system. We did, however, extract fluids from the system in order to maintain a constant pressure of 3 kbar. Greenwood's model (1975) included extraction of fluid even though he considered that a closed system case. We started this simulation with four solid phases present (dolomite, quartz, calcite, and talc with volume fractions of 0.7092, 0.07044, 0.09705, and 0.11930, respectively, compared with the bulk volume). This choice of parameters results in a fluid porosity fraction of 4×10^{-3} for the initial system. [Note that a minute quantity of tremolite was present as "seed crystals" to avoid dealing with nucleation problems].

We started the simulation with the temperature slightly higher (485 °C), and an X_{CO2} slightly lower ($X_{CO2}=0.46$), than that of the invariant point. Thus, the simulation started in the tremolite stability field. Fig. 4 summarizes the evolution of the system. The thick solid curve in Fig. 4a shows the evolution in T-X space. The curve has time stamps that are equally spaced in time indicated by successively larger circles. The area of the circles is proportional to the elapsed time. The square in the plot indicates the initial condition. The thin lines represent the equilibrium curves for reactions (1) through (5). Solid lines indicate the stable portions and dashed lines represent the metastable extensions of the equilibrium curves. As is also shown in Fig. 4b, c, the temperature falls continuously due to the endothermic nature of the reactions, while the X_{CO2} first rapidly rises, and then falls while the invariant point is approached (Lasaga et al. 2000).

One can readily see in Fig. 4a that the final approach to the invariant point for this case proceeds with reactions (1) and (4) running backward, while reactions (2), (3), and (5) run forward (cf. Table 1). This is more clearly indicated in Fig. 4d, which shows the reaction rates as a function of time. Fig. 4e shows the conversion of the solid phases, i.e., the evolution of the modal fraction of dolomite, calcite, quartz, talc, and tremolite ($V_{mineral}/V_{solids}$) as well as the porosity fraction (V_{fluid}/V_{total}). Both of these are shown on a logarithmic scale. Overall, tremolite and a minor amount of quartz are produced while there is some consumption of calcite and talc. There are indiscernible increases of the modal fraction of dolomite.

Figure 4f shows the rate of fluid production. Initially, there is rapid consumption of H_2O (solid curve starts below zero) and production of CO_2, (dashed curve starts above zero) which lead to the rapid initial increase in X_{CO2}. During the time that reaction (1) runs backwards, both H_2O and CO_2 are produced. It is of considerable interest to plot the evolution of the molar rate of production of CO_2 versus that of H_2O, as shown in Fig. 4g. The evolution begins in the upper left part of the plot, where the slope of the line is consistent with the stoichiometry of reaction (1). This branch of the curve represents only a short period of time. Most of the time is spent along the branch with a positive slope near, but not at, the slope defined by the CO_2 : H_2O ratio of the invariant point. Fig. 4h shows the ratio of CO_2 to H_2O production rates [solid curve], along with the extant CO_2 to H_2O ratio [$r=X_{CO2}/(1-X_{CO2})$, long dash signature] and the ratio implied by the invariant point composition [$r_{iip}=X_{CO2iip}/(1-X_{CO2iip})$, short dash signature]. Contrary to what was proposed by Greenwood (1975) and elaborated upon by Rice and Ferry (1982), the fluid produced does not have the composition of the invariant point composition. In fact, in order to approach the invariant point in a situation where the reaction rates become slower and slower, the produced

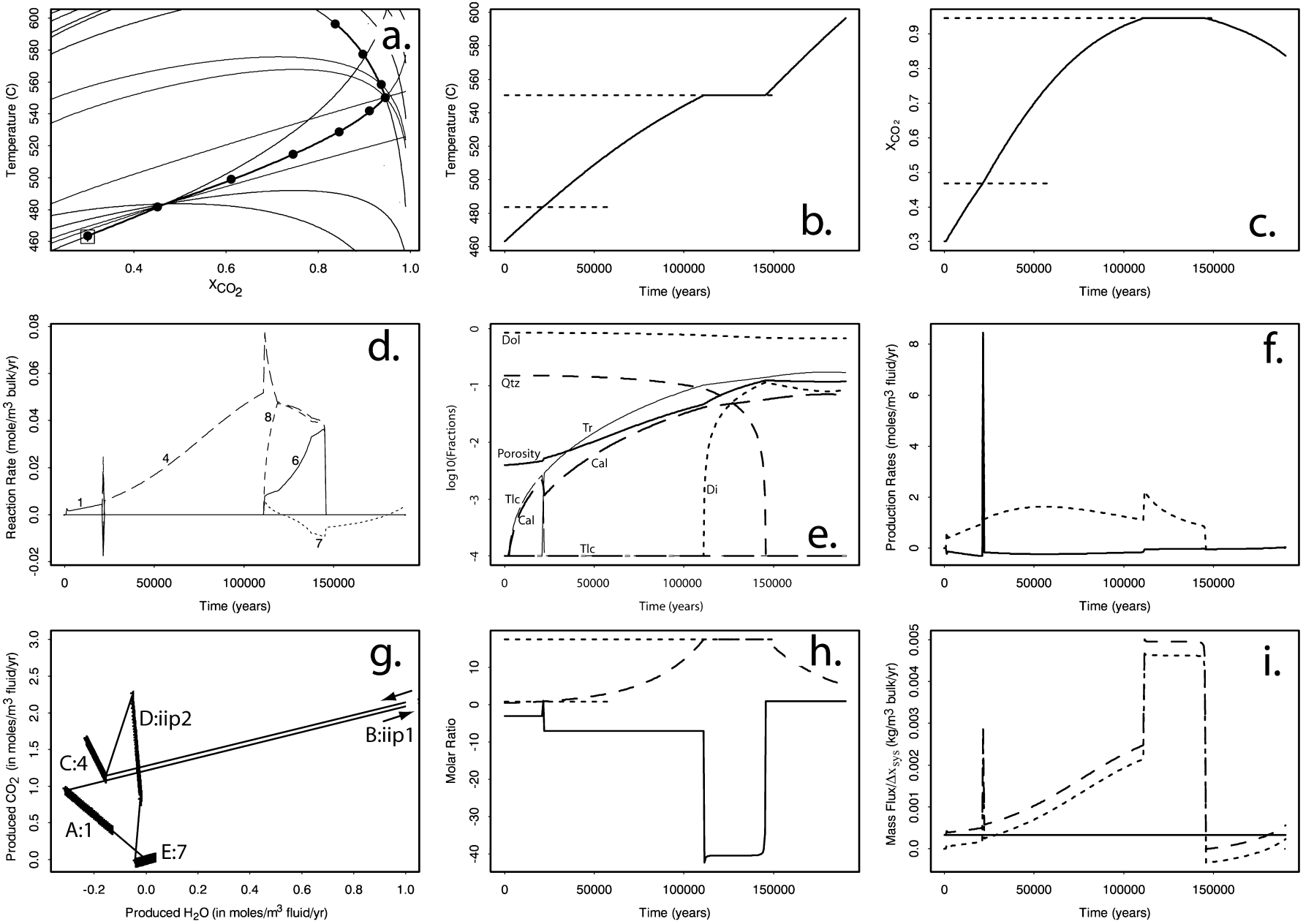
a.
Temperature (C)
X_{CO_2}
b.
Temperature (C)
Time (years)
c.
X_{CO_2}
Time (years)
d.
Reaction Rate (mole/m^3 bulk/yr)
1
4
8
6
7
Time (years)
e.
log10(Fractions)
Dol
Qtz
Tr
Porosity
Cal
Tlc
Cal
Di
Tlc
Time (years)
f.
Production Rates (moles/m^3 fluid/yr)
Time (years)
g.
Produced CO_2 (in moles/m^3 fluid/yr)
D:iip2
B:iip1
C:4
A:1
E:7
Produced H_2O (in moles/m^3 fluid/yr)
h.
Molar Ratio
Time (years)
i.
Mass Flux/Δx_{sys} (kg/m^3 bulk/yr)
Time (years)

◀

Fig 7 Simulation with external heating: heat is injected (rate equivalent of 1 °C/1,000 years), fluid injection (fluid pore velocities) of $v = 10^{-4}$ m/year; see text for detailed discussion. In part **a**, *circles* are placed at equally spaced time intervals (two circles are overlaid near the second invariant point). In part **g**, the letters *A*, *B*, *C*, *D*, and *E* indicate the sequential order of the locations visited during the simulation, while the *numbers* indicate which reactions are producing fluid (H_2O is consumed by some of the reactions). The *thin lines* (and *arrows*) indicate path connections, whereas the *thick lines* indicate actual fluid production during the evolution. Near the first invariant point, the rate of fluid production is off scale (indicated by B: iip1). Near *D* in this figure part, several reactions run near the second invariant point. See also caption of Fig. 4

fluid composition must be on the opposite side of the invariant point compared to the extant fluid composition. This is clearly evident in the figure (the extant fluid approaches that of the invariant point composition via fluid production at a smaller ratio). As we wished to maintain constant pressure in our simulations, we extracted excess fluid (visualized in Fig. 4i). Without fluid injection, the rate of extraction of fluid mass is essentially the same as the rate of production (as the composition is nearly constant).

We now consider cases with external heating. We supply heat in units of Joules/bulk volume [in m^3]/sec, but given the density and specific heat of the rock we can express the injection of heat in the more intuitive units of [°C/year], i.e. the rate that the rock would increase in temperature if there were no heat being consumed or produced by reactions. Given the endothermic nature of the decarbonation reactions, the prograde heating histories presented in some simulations may be less than the "rate equivalent" units given for heat injection (Walther and Orville 1982). Our first simulation with external heating injects heat at a rate equivalent of 1 °C/10^3 year, while no fluid is injected. Fig. 5 shows a summary of this simulation around the invariant point. Initial volume fractions (compared with the bulk volume) of dolomite and quartz for all the remaining cases were specified as 0.846 and 0.15, respectively, making the initial fluid porosity fraction 4×10^{-3} as before. Fig. 5a shows the *T*-*X* evolution of the system, and Fig. 5b indicates that the temperature does not pause in the vicinity of the first invariant point. Fig. 5d shows that reaction (1) runs forward early on, and reaction (4) proceeds later in the evolution, as would be expected from the traditional view of metamorphic petrology. Near the time when the system is close to the invariant point, several reactions run forward, while others run backwards. Of particular interest is the detailed view of the reaction rates shown in Fig. 5d. For a brief period of time, when $T > T_{IIP}$ and $X \sim X_{IIP}$, all reactions run forward (t is about 21,000 years). Soon after this, reaction (1) begins to run backwards, as does reaction (4) eventually (cf., the dips in Fig. 5a). The largest rate of fluid production (both CO_2 and H_2O as in Fig. 5f) occurs with reactions (1) and (4) running backwards, while reactions (2), (3), and (5) run forwards ($t \sim 21{,}150$ years in Fig. 5d). We note that the increased reaction rates occur "above and to the right" of the invariant point in the *T*-*X* view of Fig. 5a. During this time Fig. 5e reveals the growth of tremolite and the destruction of talc. Only a small amount of talc is produced early on, and it is "replaced" by tremolite. The apparent loss of calcite is artificial. Calcite grains actually grew, but the porosity loss was such that the modal fraction of calcite decreased. The more substantial loss of dolomite and quartz was not apparent on the logarithmic scale of modal fraction. As the rates of reactions (1), (2), (3), and (5) vanish, reaction (4) again runs forward (see Fig. 5d).

Although most of the time H_2O is consumed while CO_2 is produced, H_2O is actually produced by reactions when the system is "near" the invariant point (Fig. 5f). Fig. 5f shows significant production of H_2O and CO_2 while the reaction rates are "fastest". Before and after this time, CO_2 is produced, while H_2O is more slowly consumed.

Figure 5g shows details of the behavior of the production rates of CO_2 and H_2O (the dots are separated by equal time intervals with the evolution up the top branch and down the lower branch). The fluid produced is richer in CO_2 than the invariant point composition (solid line). Another view of the fluids produced is the ratio of CO_2 to H_2O shown in Fig. 5h (solid line) along with the extant ratio (dashed line). The apparent divergence of the fluid production ratio is only indicative of vanishing H_2O production. Fig. 5i indicates that in order to maintain constant pressure, fluid must be extracted from the system, especially during the transition near the invariant point.

As we have discussed above, each overall reaction has a rate-limiting mineral, i.e., the mineral with the smallest surface area (normalized by stoichiometry) at a given time, and the evolution of which mineral limits the rate of a given reaction can be quite complex. Fig. 6 shows which mineral limits the rate of each of the five reactions for the same time period discussed above when the system passes near the invariant point. When a given reaction is not running, we indicate zero on these curves.

The rate of reaction (1) is first limited by calcite, but talc is limiting before reaction (1) ceases. Reaction (2) is limited by tremolite, then calcite, and finally talc. The other reactions are not always limited by the same minerals. Even the switching times differ. Such complex switching among the minerals that limit the reaction rate is quite remarkable for such a simple formulation of surface area control of reaction rates, yet something analogous to this is likely an important feature of natural systems. The last part of Fig. 6 shows the evolution of ΔG_k for the first five reactions. By comparing this figure with Fig. 5d, one can deduce the critical importance of mineral surface areas in limiting the rates of reaction (even though the reaction rates have linear dependence upon ΔG_k, the actual rates of reaction are modulated by the "limiting" minerals).

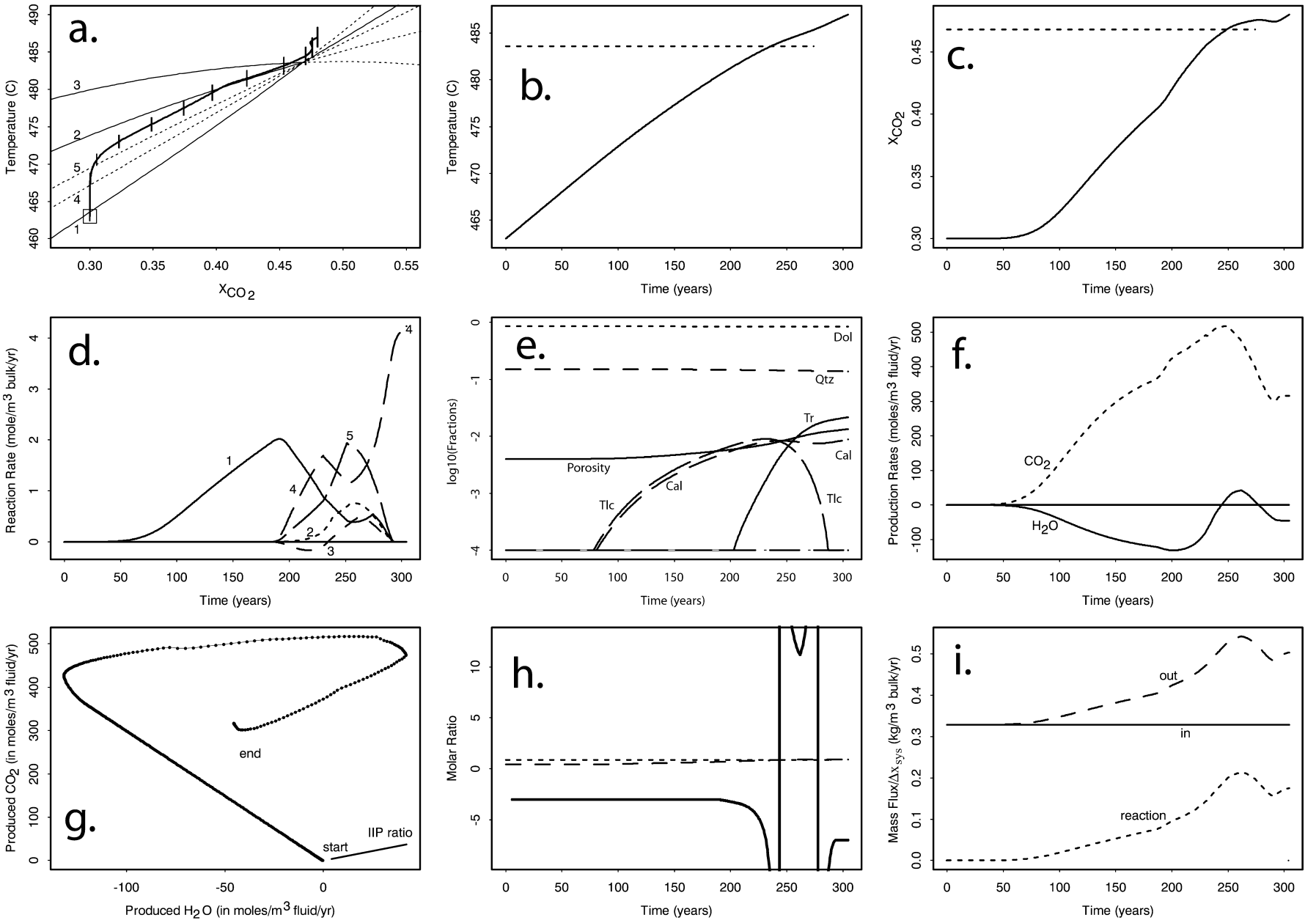
a.
Temperature (C)
X_{CO_2}
1
2
3
4
5
b.
Temperature (C)
Time (years)
c.
X_{CO_2}
Time (years)
d.
Reaction Rate (mole/m3 bulk/yr)
Time (years)
e.
log10(Fractions)
Dol
Qtz
Tr
Cal
Porosity
Cal
Tlc
Tlc
Time (years)
f.
Production Rates (moles/m3 fluid/yr)
CO_2
H_2O
Time (years)
g.
Produced CO_2 (in moles/m3 fluid/yr)
Produced H_2O (in moles/m3 fluid/yr)
end
start
IIP ratio
h.
Molar Ratio
Time (years)
i.
Mass Flux/Δx_{sys} (kg/m3 bulk/yr)
out
in
reaction
Time (years)

◄

Fig 8 Simulation with external heating: heat is injected (rate equivalent of 1 °C/10 years), fluid injection (fluid pore velocities) of $v = 10^{-1}$ m/year; see text for detailed discussion. In part **a**, *vertical bars* are placed at equally spaced time intervals. See also caption of Fig. 4

Injection with constant X_{CO2}

We now turn to simulations with fluid injected into the system. Although without fluid injection (cases discussed above) the system size was not important, if we wish to relate our work to cases with prescribed input fluxes we must specify a system size. For the purposes of this study, we chose a cube with side dimensions of 1 m (cf. Lasaga et al. 2000). We first consider the equivalent heating rate of 1 °C/10^3 years in the absence of endothermic effects. We specify an input pore velocity as an initial condition. For this case we chose an extremely slow initial velocity ($v_{pore} = 1\times10^{-4}$ m/year) and a composition $X_{CO2} = 0.3$. Admittedly, this is quite far from the range of values to which the X_{CO2} of the system evolves (this would thus involve large spatial gradients in fluid composition, as our system size in 1 m). The input pore velocity coupled with the composition was converted into an input molar flux using the porosity and average molar volume of the fluid. Throughout the simulation, the input molar flux was held constant. Given changing porosity and fluid density, the actual pore velocity varied somewhat during the simulations, while the input Darcy velocities changed only slightly. These caveats should be kept in mind when heating and injection rates are described below.

Figure 7a, b, and c show the evolution of the temperature and X_{CO2} for the conditions just described. The behavior around the first invariant point is similar to the previous case described in detail, i.e., reaction (1) first produces a small amount of talc that is destroyed by simultaneous forward and backward reactions near the first IIP (cf. also Fig. 7d, e). Reaction (4) then produces calcite and tremolite at the expense of dolomite and quartz. The system eventually passes slightly above the second IIP (near $T\sim550$ °C and $X_{CO2}\sim0.946$). During this trajectory, reactions (8), (6), and (7) "turn on" in succession, each producing diopside, while the quartz is being consumed. As is evident by comparing Fig. 7a, b, and c, the system remains close to the second IIP for a period of time (the invariant point is overstepped by a scant 0.01 °C for nearly 50 ka). During this time, the overall effect of the reactions [primarily reactions (4) and (8) in the early phase near this IIP] is to consume H_2O and to produce CO_2. This is somewhat balanced by the continuous injection of H_2O rich fluid, which helps to keep X_{CO2} nearly constant. Eventually, reaction (6) (which produces H_2O) grows in amplitude, while reaction (7) reverses direction. Quartz is finally used up so that reactions (4), (6), and (8) all stop. Subsequently the combination of heating and injection permit reaction (7) to run forward again. In the early stage of the fluid production, shown in Fig. 7f, the rates of H_2O consumption and production are small compared to that of CO_2, except near the first IIP. Figure 7g is the plot of net CO_2 production versus that of H_2O. Starting from the origin, the system moves up the low negative slope branch [slope −3 for reaction (1)], then proceeds far off scale to the right near the first IIP, then moves to the next steeper negative slope [-7 for reaction (4)], then to the very steep negative slope during the transition near the second IIP [primarily a combination of reactions (4) and (8), with some effect from reactions (6) and (7)], and then to the zone near the origin [with slope 0.5 corresponding to reaction (7)]. Much of the time dependence of these production slopes can be extracted from Fig. 7h, where the values of the production ratio correspond to the slopes of Fig. 7g. (The short dashed lines in Fig. 7h correspond to the CO_2 to H_2O ratios at the invariant points).

The mass flux (divided by the system size Δx_{sys}) into and out of the system is shown in Fig. 7i, by the solid and long-dashed lines, respectively. Recall that the system size is 1 m^3. The face receiving fluid injected has an area of 1 m^2. The distance from the receiving face to the effluent face is $\Delta x_{sys} = 1$ m. Also shown by short dashes is the rate of mass production per volume in the system, which dips slightly negative when reaction (7) is backwards (fluid is then consumed). One remarkable feature illustrated by this plot is that much more fluid is generally produced in this 1 m^3 box than was injected!

The implications of this massive fluid production are profound, and have often been noted in the literature. Namely, it can be expected that metamorphic decarbonation reactions can produce so much fluid that the rock might be expected to break and that crack networks could be necessary to carry the fluids away (cf. Ague et al. 1998; Walther and Orville 1980, 1982). The highly variable nature of the net fluid production is also remarkable. It depends on the fluid injection and the rate of heating in a delicate way.

The case discussed above represents a scenario of slow heating rate combined with a very slow fluid flow rate and relatively fast intrinsic reaction rates derived from experimental work (e.g., Schramke et al. 1987). The resulting path in the T-X diagram is close to paths resulting from common equilibrium scenarios, even though the detailed behavior is complex. This result demonstrates that our kinetic model allows for an equilibrium scenario as an endmember case. However, with a number of cases, Lasaga et al. (2000) have shown that near equilibrium behavior is not very likely if flow rates are reasonably fast, even if the heating rates are slow. In the following simulations we will show some scenarios similar to contact metamorphic conditions that cause even larger deviations from equilibrium.

Figure 8 shows the results for pore fluid velocities of $v = 10^{-1}$ m/year, but a heating rate (1 °C/10 year). Figure 8a indicates drastic overstepping of first reaction (1), and subsequently sequential overstepping of reactions (4), (5), (2), and (3), by the time the invariant point composition is reached. There is a rather interesting

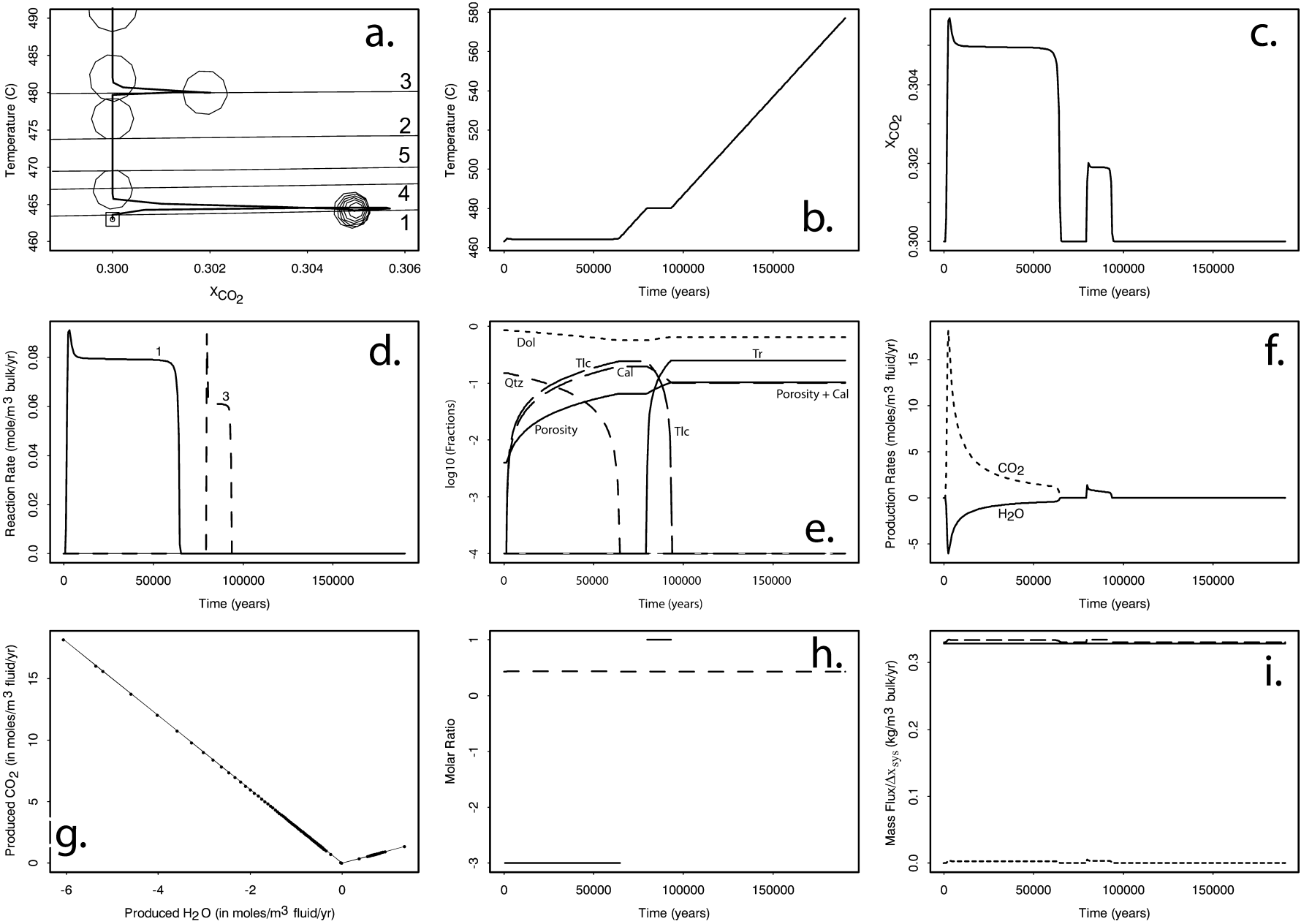
a.
Temperature (C)
X_{CO_2}
3
2
5
4
1
b.
Temperature (C)
Time (years)
c.
X_{CO_2}
Time (years)
d.
Reaction Rate (mole/m3 bulk/yr)
1
3
Time (years)
e.
log10 (Fractions)
Dol
Tlc
Cal
Tr
Qtz
Porosity + Cal
Porosity
Tlc
Time (years)
f.
Production Rates (moles/m3 fluid/yr)
CO_2
H_2O
Time (years)
g.
Produced CO_2 (in moles/m3 fluid/yr)
Produced H_2O (in moles/m3 fluid/yr)
h.
Molar Ratio
Time (years)
i.
Mass Flux/Δx_{sys} (kg/m3 bulk/yr)
Time (years)

◀

Fig 9 This case considers the same flow rate as in Fig. 8 (initial pore velocities of injection is 10^{-1} m/year) but a much slower heating rate equivalent of 1 °C/1,000 years; see text for detailed discussion. In part **a**, *circles* of increasing radii with time are placed along the path, separated by equal times, with *T-X* evolution changing more slowly just after passing reaction curves *1* and *3* (not near the invariant point). See also caption of Fig. 4

story embedded in which reactions could run forward or backward compared with what is actually observed in Fig. 8d. The times at which reactions are overstepped were calculated and they are: reaction (1): 5.5 years, (4): 41.5 years, (5): 67 years, (2): 185 years, and finally (3): 234 years. Reaction (1) starts slowly, gradually building up talc and calcite. Noticeable quantities of these minerals become apparent in Fig. 8e by 80 years into the simulation. Then there is a sudden onset of reaction (4) and other reactions. This timing is not precisely associated with the crossing of any of the reaction curves. Reaction (4) and (5) start running forward at $t = 179$ years. At the same time, reactions (2) and (3) begin running in reverse [somewhat later, first reaction (2), and then (3), run forward when their univariant curves are crossed]. This surprising behavior may be explained on the basis of how the reaction rates depend not only on the deviation from equilibrium, but also upon the mineral surface areas and the possibility of simultaneous stable and metastable reactions running in either direction (depending on their ΔG's). As soon as reaction (4) is crossed, it would be possible to form tremolite. However, this could trigger reactions (2), (3), and (5) to run in the reverse direction. Tremolite would be the "limiting mineral" for each of these reactions (i.e., its surface area would be so small that, of all the other mineral areas, the surface area of tremolite would control the rates of the overall reactions, of course moderated by the ΔG's of reaction).

It turns out that the growth rate (change of size with time) of a "limiting" mineral due to a given reaction is independent of its surface area, even though the overall reaction rate depends on that surface area (see discussion in Lasaga 1984, 1998). Therefore, the growth rate of the limiting mineral due to a particular reaction depends only on the temperature and the deviation from equilibrium for that reaction. When several competing reactions are involved, some of which would run forward and others would run backwards, the net effect could be that any amount of mineral formed by one reaction would be destroyed by another reaction. This tendency disallows the formation of tremolite until the combination of reactions makes its growth feasible. This need not happen at the crossing point of any particular reaction, but depends instead upon the delicate balance of various ΔG's of reaction. Figure 8d shows the dominant reaction rates for reactions 2–5 turn on together. The net effect is tremolite formation, which is soon noticeable in Fig. 8e, whereas only reaction (4) runs once talc is consumed.

Figure 8f, g, h, and i shows various aspects of the fluid production for this case. Figure 8g indicates a much richer structure of fluid production than can be explained by the stoichiometry of single reactions, and Fig. 8h shows fluid production far from the invariant point composition. Figure 8i indicates significant fluid production occurs within the 1 m^3 volume, so that flux increases at this scale would be significant.

We now briefly mention a case whose results show greater importance of the injected fluid. This case considers initial pore velocities of injection of 10^{-1} m/year. Fig. 9 shows the results for the equivalent heating rates (if it were not for reaction enthalpy effects) of 1 °C/1,000 years. The plateaus of temperature and CO_2, especially when reaction (1) is overstepped, are related to the concept of steady states discussed in Lasaga et al. (2000, 2001). The picture is also similar to the dotted path of Fig. 16–8 in Philpotts (1990). Of course there are differences as we observe slight shifts in the fluid compositions, and the "steady states" are slightly displaced from the equilibrium curves (which in fact should influence the calculation of the amount of fluids produced). Figure 9d indicates that the reaction rates can nearly achieve a steady state until one of the phases is consumed. Figure 9e shows the complete consumption of quartz by 70,000 years into the simulation, during which time significant gains in talc and calcite abundance are observed [all due to reaction (1)]. Later, reaction (3) is overstepped slightly. Endothermic effects again tend to hold the temperature steady while tremolite is formed at the expense of talc [a more precise statement is given by the stoichiometry of reaction (3)]. The CO_2 production and the H_2O consumption and production are consistent with these reactions, as illustrated in Fig. 9f, g, and h. The comparison of fluid production to the input and output "fluxes" shown in Fig. 9i indicate that for these conditions, the local fluid production rate is small compared with what is injected. Therefore, pressure build up that is sufficient to induce rock fracture would not be expected with these conditions. Compared with the case discussed in detail just above, the temperature oversteps are quite small and the fluid composition returns to the input composition quickly after mineral phases are consumed. The temperature evolution has two plateaus (Fig. 9b), but the fluid compositions and the reaction rates (Fig. 9c and d, respectively) are a bit more rounded, and less like a true steady state.

Our model results show that kinetic concepts help elucidate our understanding of metamorphic reactions that include (de)volatilization. All petrogenetic grids (*T-X* diagrams) that are used to interpret metamorphic rocks should include the metastable extensions of all equilibrium curves involved. Additionally, there may be a larger number of reactions that need to be considered to gain a complete picture. Metastable mineral reactions, like reaction (5) (see Fig. 1 and Table 1), must also be included. Many reactions can run forward or backward producing apparent stoichiometries that vary with time. The reason for the addition of metastable

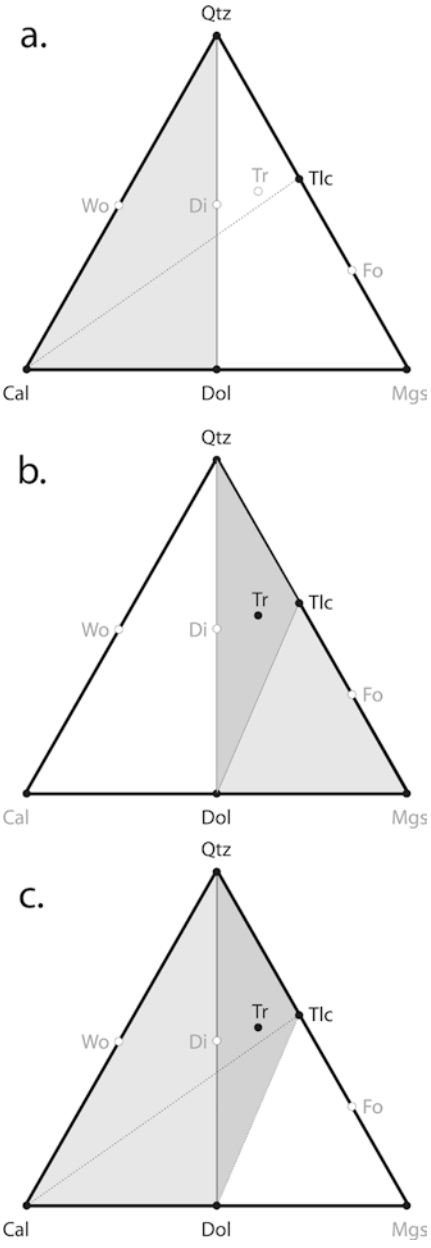

Fig 10 A sequence of phase diagrams for the CMS system. **a** Reaction (1) 3 Dol + 4 Qtz + 1 $H_2O \Leftrightarrow$ 1 Tlc + 3 Cal + 3 CO_2 in the left half of the triangle Cal-Dol-Qtz. **b** reaction (5) 1 Tlc + 2 Dol + 4 Qtz $\Leftrightarrow$ 1 Tr + 4 CO_2 is allowed only in the right half of the triangle (Dol-Mgs-Qtz) if the equilibrium thermodynamic concept is applied. **c** reaction (1) and (metastable) reaction (5) can occur at the same time if we apply the kinetic concept and conditions are forcing the overstep of both univariant curves. *Cal* calcite, *Di* diopside, *Dol* dolomite, *Fo* forsterite, *Qtz* quartz, *Tlc* talc, *Tr* tremolite, *Wo* wollastonite, *Mgs* magnesite)

reaction (5) will become obvious in the following discussion.

Let us consider reaction (5) in the CMS system.

$$2 \text{ dolomite} + 4 \text{ quartz} + 1 \text{ talc} \Leftrightarrow 1 \text{ tremolite} + 4\ CO_2.$$

This reaction could not occur if we would apply only the equilibrium concept. The reason is that there is no scenario that would allow the production of the mineral assemblage dolomite–quartz–talc (see Fig. 10a). And, therefore, reaction (5) would not be a valid mineral reaction in the left half of the CMS system (i.e., calcite–dolomite–quartz). The reaction path predicted by the equilibrium concept could deviate from reaction (1) only if one of the reactants (dolomite or quartz) is depleted. The above assemblage could exist in the other half of the CMS system only, i.e., dolomite–magnesite–quartz (Fig. 10b). Here reaction (5) is considered a stable reaction.

The assemblage dolomite–quartz–talc is a valid one if we apply the concept of reaction kinetics. A heating rate that is fast enough relative to the reaction rates will force the system to overstep not only reaction (1), but also reaction (5) (see Fig. 8a). In this case, reaction (1) would produce talc (and calcite) from dolomite and quartz. The three reactants necessary for reaction (5) are present and can form tremolite if reaction (5) becomes overstepped as well (Fig. 10c). Consequently, reaction (5) must be considered, because it will significantly influence the development of the system. We can metastably produce tremolite left of the first isobaric invariant point, i.e., at lower temperatures and in the presence of a fluid phase that is significantly richer in H_2O than usually expected. This new scenario would be unthinkable if we had strictly followed equilibrium thermodynamics.

Summary and conclusion

Thermodynamic petrologic models have been well developed during the last 100 years. Models to explain the interactions of rocks with mixed-volatile fluids have relied heavily on equilibrium thermodynamics. The concept of "buffering" requires that the kinetics of metamorphic reactions are fast enough that the rocks maintain all fluids at equilibrium. However, available kinetic data for several metamorphic reactions indicate that, in systems open to fluids, equilibrium may not be achieved. It is commonly assumed that equilibrium was achieved in a metamorphic system if the correct number of phases is present. The phase rule can predict the number of phases present at equilibrium. However, the number of phases present in a rock is not a test of equilibrium. For instance, as shown, the number of phases required for equilibrium at an invariant point can also be achieved by overstepping of any combination of two or more univariant stable or metastable reactions that are common to a given invariant point.

The possible reaction pathways of metamorphic systems can be significantly different from the pathways predicted by the thermodynamic approach. Importantly, in the kinetic approach, pathways are likely to include metastable reactions. A pervasive argument in proving that equilibrium thermodynamic models are applicable is the consistency of the mineral assemblage pattern found in nature to the pattern predicted by thermodynamics. This paper demonstrates that a given pattern of

occurrence of mineral assemblages can be produced by an unlimited number of kinetic *P-T-X* pathways, thus demonstrating that mineral occurrence alone cannot be used to verify equilibrium.

Our case studies show a few examples of possible kinetic pathways that result from the variations in the heating and fluid flow rates expected in natural metamorphic systems. This range includes situations where the fluid composition remains fairly close to the equilibrium curve of one or more overall reactions and situations where the fluid composition is significantly out of equilibrium with any overall reaction. Certainly, the degree of disequilibrium depends on the details of the rates of heating, fluid flow, and reactions.

By using petrologic models with kinetic concepts, a detailed understanding of metamorphism depends critically on reliable kinetic data. In the future, it will be a key challenge to produce those data, as well as solubility data for CO_2-H_2O mixtures.

Acknowledgments The authors want to thank J.J. Ague, M.J. Davis, P. Metz, N.M. Ribe, D. Rosner, R. Rye, J. Sisson, B.J. Skinner, and G. Veronis for helpful discussions. We also acknowledge R.F. Dymek, C.E. Manning, J.V. Walther, Tom Torgersen, and G.M. Dipple for critical, but helpful, comments and careful reviews of drafts of an earlier manuscript from which this version has evolved. We also thank J.M. Ferry and R. Milke for careful reviews and thoughtful comments, as well as editorial handling by J. Hoefs. Thanks also goes to A.C. Lasaga. EWB and AL would like to thank him for discussions regarding methods for calculation of enthalpies, Gibbs free energies, fugacities, composition evolution, and standard states of gases and minerals. Parts of the study were funded by the Department of Energy (DE-FG02-90ER14153, DE-FG02-01ER15216, DE-FG03-02ER63427, and DE-FG07-01R63295), the National Science Foundation (grants EAR-9628238, EAR-9526794, EAR-9727134, EAR-0125667), the Alexander von Humboldt-Foundation, EXXON MOBIL Upstream Research Productions, and the Schlumberger-Doll Research in Ridgefield, Connecticut.

References

Ague JJ, Park JJ, Rye DM (1998) Regional metamorphic dehydration and seismic hazard. Geophys Res Lett 25:4221–4224

Ague JJ, Rye DM (1999) Simple models of CO_2 release from metacarbonates with implications for interpretation of directions and magnitudes of fluid flow in the deep crust. J Petrol 40:1443–1462

Balashov VN, Yardley BWD (1998) Modeling metamorphic fluid flow with reaction-compaction-permeability feedbacks. Am J Sci 298:441–470

Baxter EF, DePaolo DJ (2000) Field measurements of slow metamorphic reaction rates at temperatures of 500 to 600 °C. Science 288:1411–1414

Baxter EF, DePaolo DJ (2002a) Field measurement of high temperature bulk reaction rates; I, Theory and technique. Am J Sci 302:442–464

Baxter EF, DePaolo DJ (2002b) Field measurement of high-temperature bulk reaction rates; II, Interpretation of results from a field site near Simplon Pass, Switzerland. Am J Sci 302:465–516

Berman RG (1988) Internally consistent thermodynamic data for minerals in the system Na_2O-K_2O-CaO-MgO-FeO-Fe_2O_3-Al_2O_3-SiO_2-TiO_2-H_2O-CO_2. J Petrol 29:445–522

Bolton EW, Lasaga AC, Rye DM (1999) Long-term flow/chemistry feedback in a porous medium with heterogeneous permeability: kinetic control of dissolution and precipitation. Am J Sci 299:1–68

Bolton EW, Lüttge A, Rye DM (2003) A model of contact metamorphism of siliceous dolomites in two dimensions (in preparation)

Burch TE, Nagy KL, Lasaga AC (1993) Free energy dependence of albite dissolution kinetics at 80 °C and pH 8.8. Chem Geol 105:137–162

Cama J, Ganor J, Ayora C, Lasaga AC (2000) Smectite dissolution kinetics at 80 °C and pH 8.8. Geochim Cosmochim Acta 64:2701–2717

Connolly JAD (1997) Devolatilization-generated fluid pressure and deformation-propagated fluid flow during prograde regional metamorphism. J Geophys Res 102/B8:18149–18173

Cui X, Nabelek PI, Liu M (2002) Numerical modeling of fluid flow and oxygen isotope exchange in the Notch Peak contact-metamorphic aureole, Utah. GSA Bull 114 (7):869–882

Dachs E, Metz P (1988) The mechanism of the reaction: 1 tremolite + 3 calcite + 2 quartz = 5 diopside + 3 CO_2 + 1 H_2O: results of powder experiments. Contrib Mineral Petrol 100:542–551

Dipple GM, Ferry JM (1992) Fluid flow and stable isotope alteration in rocks at elevated temperatures with applications to metamorphism. Geochim Cosmochim Acta 56:3539–3550

Ernst WG, Banno S (1991) Neoplastic jadeitic pyroxene in Franciscan metagreywackes from Pacheco Pass, central Diablo Range, California, and implications for the inferred metamorphic P-T trajectory. N Z J Geol Geophys 34:285–292

Eskola P (1915) On the relation between chemical and mineralogical composition in the metamorphic rocks of the Orijärvi region. Bull Commun Geol Finland 40

Ferry JM (1986) Reaction progress: a monitor of fluid-rock interaction during metamorphic and hydrothermal events. In: Walther JV, Wood BJ (eds) Fluid-rock interactions during metamorphism. Springer, Berlin Heidelberg New York, pp 60–88

Ferry JM (1991) Dehydration and decarbonation reactions as a record of fluid infiltration. In: Kerrick DM (ed) Mineralogical Society of America, Revs Mineral 26:351–394

Ferry JM, Dipple GM (1991) Fluid flow, mineral reactions, and metamorphism. Geol 19:211–214

Ferry JM, Dipple GM (1992) Models for coupled fluid flow, mineral reaction, and isotropic alteration during contact metamorphism: the Notch Peak aureole, Utah. Am Min 77:577–591

Ferry JM, Wing BA, Penniston-Dorland SC, Rumble D III (2002) The direction of fluid flow during contact metamorphism of siliceous carbonate rocks: new data for the Monzoni and Predazzo aureoles, northern Italy, and a global review. Contrib Mineral Petrol 142:679–699

Gibbs JW (1878) On the equilibrium of heterogeneous substances. Am J Sci 16:441–458

Giorgetti G, Tropper P, Essene EJ, Peacor DR (2000) Characterization of non-equilibrium and equilibrium occurrences of paragonite/muscovite intergrowths in an eclogite from the Sesia-Lanzo Zone (Western Alps, Italy). Contrib Mineral Petrol 138:326–336

Gottschalk M (1997) Internally consistent thermodynamic data for rock forming minerals. Eur J Min 9:175–223

Greenwood HJ (1975) Buffering of pore fluids by metamorphic reactions. Am J Sci 275:573–593

Heinrich W, Metz P, Bayh W (1986) Experimental investigation of the mechanism of the reaction: 1 tremolite +11 dolomite = 8 forsterite + 13 calcite + 9 CO_2 + 1 H_2O. Contrib Mineral Petrol 93:215–221

Heinrich W, Metz P, Gottschalk M (1989) Experimental investigation of the kinetics of the reaction: 1 tremolite +11 dolomite = 8 forsterite + 13 calcite + 9 CO_2 + 1 H_2O. Contrib Mineral Petrol 102:163–173

Heuss-Aßbichler S, Masch L (1991) Microtextures and reaction mechanism of carbonate rocks: a comparison between the thermoaureoles of Ballachulish and Monzoni (N. Italy).

Equilibrium and kinetics in contact metamorphism, 1st edn. Springer, Berlin Heidelberg New York, pp 229–249
Hewitt DA (1973) The metamorphism of micaceous limestones from south-central Connecticut. Am J Sci 273A:444–469
Jacobs GK Kerrick DM (1981) APL and FORTRAN programs for a new equation of state H_2O, CO_2 and their mixtures at supercritical conditions: Comp Geosci 7/2:131–143
Jordan G, Metz P, Lüttge A (1992) Metastabile Talkbildung im Tremolit-Stabilitätsfeld. Fortschr Min Beih z Eur J Mineral 4:136
Käse H-R, Metz P (1980) Experimental investigation of the metamorphism of siliceous dolomites. Contrib Mineral Petrol 73:151–159
Kerrick DM (1990) The Al_2SiO_5 Polymorphs. Min Soc Am Rev Miner 22
Kerrick DM, Jacobs GK (1981) A modified Redlich-Kwong equation for H_2O, CO_2 and H_2O-CO_2 mixtures at elevated pressures and temperatures: Am J Sci 281:735–767
Kerrick DM, Lasaga AC, Raeburn SP (1991) Kinetics of heterogeneous reactions. In: Kerrick DM (ed) Min Soc Am Rev Miner 26:583–671
Korzhinskii DS (1950) Equilibrium factors in metasomatism. Izv Akad Nauk SSSR, Ser Geol no 3
Korzhinskii DS (1957) Physicochemical basis of the analysis of the paragenesis of minerals. Academy of Sciences Press, Moscow (English translation by Consultants Bureau, Inc. New York, 1959)
Korzhinskii DS (1966) On thermodynamics of open systems and the phase rule (a reply to DF Weill and WS Fyfe). Geochim Cosmochim Acta 30:829–835
Korzhinskii DS (1967) On thermodynamics of open systems and the phase rule (a reply to the second critical paper of D.F. Weill and W.S. Fyfe). Geochim Cosmochim Acta 30:1177–1180
Kridlebaugh SJ (1971) Kinetics of calcite + quartz = wollastonite + carbon dioxide at high pressures and temperatures. Trans Am Geophys Union 52:378
Kridlebaugh SJ (1973) Kinetics of calcite + quartz = wollastonite + carbon dioxide at high pressures and temperatures. Am J Sci 273:757–777
Lasaga AC (1984) Chemical kinetics of water-rock interactions. J Geophys Res 89:4009–4025
Lasaga AC (1986) Metamorphic reaction rate laws and the development of isograds. Mineral Mag 50:359–373
Lasaga AC (1998) Kinetic theory in Earth sciences. Princeton Press, Princeton, 811 pp
Lasaga AC, Rye DM (1993) Fluid flow and chemical reactions in metamorphic systems. Am J Sci 293:361–404
Lasaga AC, Lüttge A, Rye DM, Bolton EW (2000) Dynamic treatment of invariant and univariant reactions in metamorphic systems. Am J Sci 300:173–221
Lasaga AC, Rye DM, Lüttge A, Bolton EW (2001) Calculations of fluid fluxes in Earth's crust. Geochim Cosmochim Acta 65:1161–1185
Lattanzi P, Rye DM, Rice JM (1980) Behavior of ^{13}C and ^{18}O in carbonates during contact metamorphism at Maryville, Montana: implications for isotope systematics in impure dolomitic limestones. Am J Sci 280:890–906
Lüttge A, Metz P (1991) Mechanism and kinetics of the reaction: 1 dolomite + 2 quartz = 1 diopside + 2 CO_2 investigated by powder experiments. In: Gordon TM, Martin RF (eds) Quantitative methods in petrology; an issue in honor of Hugh J Greenwood. Can Mineral 29:803–821
Lüttge A, Metz P (1993) Mechanism and kinetics of the reaction: 1 dolomite + 2 quartz = 1 diopside + 2 CO_2: a comparison of rock-sample and of powder experiments. Contrib Mineral Petrol 115:155–164
Lüttge A, Bolton EW, Rye DM, Lasaga AC (1997a) Kinetic control of metamorphic isograd. GSA 1997 annual meeting, abstracts 29:A94
Lüttge A, Bolton EW, Rye DM, Lasaga AC (1997b) Kinetics vs. thermodynamic equilibrium: control on the occurrence of metamorphic isograds. Berichte der Deutschen Mineralogischen Gesellschaft, Beih Europ J Mineral 9/1
Lüttge A, Neumann U, Lasaga AC (1998) The Influence of heating rate on the kinetics of mineral reactions: an experimental study and computer models. Am Mineral 83:501–515
Lüttge A, Bolton EW, Lasaga AC (1999) An interferometric study of the dissolution kinetics of anorthite: the role of reactive surface area. In:Canfield D, Boudreau B (eds) Biogeochemical cycles and their evolution over geologic time. A special triple issue as a tribute to the career of Robert A. Berner. Am J Sci 299:652–678
Manning CE, Ingebritsen SE, Bird DK (1993) Missing mineral zones in contact metamorphosed basalts. Am J Sci 293:894–938
Masch L, Heuss-Aßbichler S (1991) Decarbonation reactions in siliceous dolomites and impure limestones. Equilibrium and kinetics in contact metamorphism, 1st ed. Springer, Berlin Heidelberg New York, pp 229–249
Matthews A, Goldsmith JR (1984) The influence of metastability on reaction kinetics involving zoisite formation from anorthite at elevated pressures and temperatures. Am Min 69:848–857
Metz P (1967) Experimentelle Bildung von Forsterit und Calcit aus Tremolit und Dolomit. Geochim Cosmochim Acta 31:1517–1532
Metz P (1970) Experimental investigation of the metamorphism of siliceous dolomites. II. The conditions of diopside formation. Contrib Mineral Petrol 28:221–250
Metz P (1976) Experimental investigation of the metamorphism of siliceous dolomites. III. Equilibrium data for the reaction: 1 tremolite + 11 dolomite↔8 forsterite + 13 calcite + 9 CO_2 + 1 H_2O for the total pressure of 3,000 and 5,000 bars. Contrib Mineral Petrol 58:137–148
Metz P, Puhan D (1970) Experimental investigation of the metamorphism of siliceous dolomites. I. The equilibrium data of the reaction: 3 dolomite + 4 quartz + 1 H_2O ↔ 1 talc + 3 calcite + 3 CO_2 determined for the total pressure of 1,000, 3,000 and 5,000 bars. Contrib Mineral Petrol 26:302–314
Metz P, Trommsdorff V (1968) On phase equilibria in metamorphosed siliceous dolomites. Contrib Mineral Petrol 18:305–309
Milke R, Metz P (2002) Experimental investigation of the kinetics of the reaction wollastonite + calcite + anorthite = grossular + CO_2. Am J Sci 302:312–345
Miyashiro A (1961) Evolution of metamorphic belts. J Petrol 2:277–311
Nagy KL, Lasaga AC (1992) Dissolution and precipitation kinetics of gibbsite at 80 °C and pH 3: the dependence on solution saturation state. Geochim Cosmochim Acta 56:3093–3111
Philpotts AR (1990) Principles of igneous and metamorphic petrology. Prentice Hall, Englewood Cliffs, New Jersey
Rice JM (1977a) Contact metamorphism of impure dolomitic limestone in the Boulder aureole, Montana. Contrib Mineral Petrol 59:237–259
Rice JM (1977b) Progressive metamorphism of impure limestone in the Marysville aureole, Montana. Am J Sci 277:1–24
Rice JM, Ferry JM (1982) Buffering, infiltration, and the control of intensive variables during metamorphism. In: Ferry JM (ed) Characterization of metamorphism through mineral equilibria. Miner Soc Am Rev Miner 10:63–326
Ridley J, Thompson AB (1986) The role of mineral kinetics in the development of metamorphic microtextures. In: Walther JV, Wood BJ (ed) Fluid-rock interactions during metamorphism. Springer, Berlin Heidelberg New York, pp 154–193
Roselle GT, Baumgartner LP, Valley JW (1999) Stable isotope evidence of heterogeneous fluid infiltration at the Ubehebe Peak contact aureole, Death Valley National Park, California. Am J Sci 299:93–138
Rubie DC (1998) Disequilibrium during metamorphism: the role of nucleation kinetics. In: Treloar PJ, O'Brien PJ (ed) What drives metamorphism and metamorphic reactions? Geol Soc Lond Spec Publ 138:199–214
Schramke JA, Kerrick DM, Lasaga AC (1987) The reaction muscovite + quartz = andalusite + K-feldspar + water, Part 1. Growth kinetics and mechanism. Am J Sci 287:517–559

Skippen GB, Trommsdorff V (1975) Invariant phase relations among minerals on T-X_{fluid} sections. Am J Sci 275:561–572

Spear FS (1995) Metamorphic phase equilibria and pressure-temperature-time paths. Min Soc Am Monogr Wash, p 799

Steefel CI, Lasaga AC (1990) Evolution of dissolution patterns. In: Melchior DC, Bassett RL (eds) Chemical modeling of aqueous systems II: ACS Symposium Series 416, Am Chem Soc, pp 212–225

Steefel CI, Lasaga AC (1992) Putting transport into water-rock interaction models. Geol 20:680–684

Steefel, CI, Lasaga AC (1994) A coupled model for transport of multiple chemical species and kinetic precipitation/dissolution reactions with application to reactive flow in single-phase hydrothermal systems. Am J Sci 294:529–592

Steefel CI, Van Cappellen P (1990) A new kinetic approach to modeling water-rock interaction: the role of nucleation, precursors, and Ostwald ripening. Geochim Cosmochim Acta 54:2657–2677

Tanner SB, Kerrick DM, Lasaga AC (1985) Experimental kinetic study of the reaction: calcite + quartz = wollastonite + carbon dioxide, from 1 to 3 kilobars and 500 to 850 °C. Am J Sci 285:577–620

Taylor AS, Blum JD, Lasaga AC (2000) The dependence of labradorite dissolution and Sr isotope release rates on solution saturation state. Geochim Cosmochim Acta 64:2389–2400

Thompson JB Jr (1955) The thermodynamic basis for the mineral facies concept. Am J Sci 253:65–103

Thompson JB Jr (1959) Local equilibrium in metasomatic processes. In: Abelson PH (ed) Researches in Geochemistry. Wiley, New York, pp 427–457

Thompson JB Jr (1970) Geochemical reaction in open systems. Geochim Cosmochim Acta 34:529–551

Tracy RJ, Hewitt DA, Schiffries CM (1983) Petrologic and stable-isotope studies of fluid-rock interactions south-central Connecticut. I. The role of infiltrations in producing reaction assemblages in impure marbles. Am J Sci 283A:589–616

Trommsdorff V (1972) Change in T-X during metamorphism of siliceous dolomite rocks of the central Alps. Schweiz Mineral Petrogr Mitt 52:567–571

van Haren JLM, Ague JJ, Rye DM (1996) Oxygen isotope record of fluid infiltration and mass transfer during regional metamorphism of pelitic schist, Connecticut, USA. Geochim Cosmochim Acta 60:3487–3504

Walther JV (1996) Fluid production and isograds reactions at contacts of carbonate-rich and carbonate-poor layers during progressive metamorphism. J Metamorph Geol 14:351–360

Walther JV, Orville PM (1980) Rates of metamorphism and volatile production and transport in regional metamorphism. Geol Soc Am, Abstr Prog 12:544

Walther JV, Orville PM (1982) Volatile production and transport in regional metamorphism. Contrib Mineral Petrol 79:252–257

Walther JV, Wood BJ (1984) Rate and mechanism in prograde metamorphism. Contrib Mineral Petrol 88:246–259

Weill DF, Fyfe WS (1964) A discussion of the Korzhinskii and Thompson treatment of thermodynamic equilibrium in open systems. Geochim Cosmochim Acta 28:565–576

Weill DF, Fyfe WS (1967) On equilibrium thermodynamics of open systems and the phase rule (a reply to D.S. Korzhinskii). Geochim Cosmochim Acta 31:1167–1176

Winkler U, Lüttge A (1999) An experimental study of the influence of $CaCl_2$ on the kinetics of the reaction: 1 tremolite + 3 calcite + 2 quartz = 5 diopside + 2 CO_2. Am J Sci 299:393–427

Yardley BWD (1993) An introduction to metamorphic petrology. Longman Earth Science Series, Longman/Wiley, New York, 248 pp